Electrohydrodynamic Propulsion Systems

To what effect does the electrode separation affect the efficiency of an ion thruster?

Candidate Code: [redacted]
Session: May 2021
Subject: Physics
Word Count: 3,994
DP Extended Essay

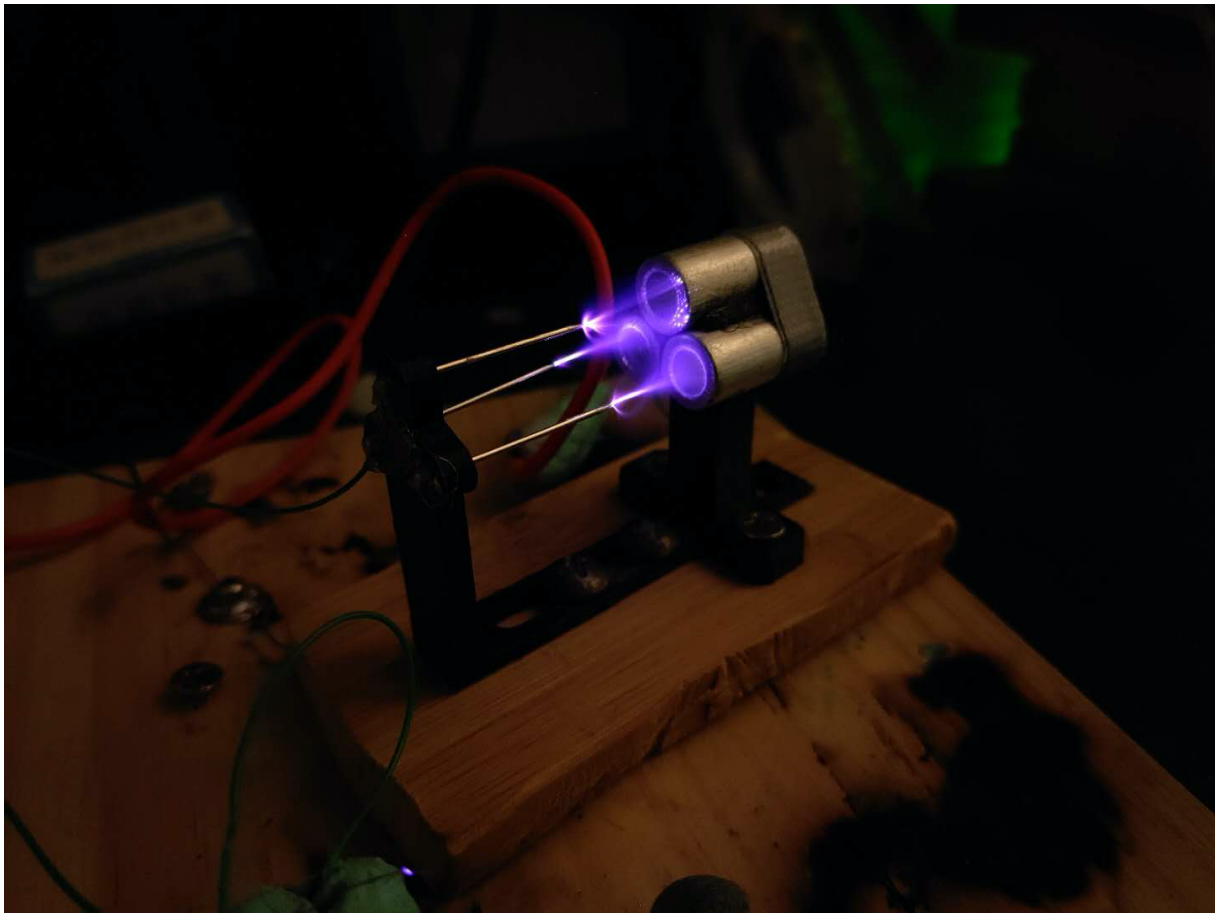

Table of Contents

1 Introduction

Having always been intrigued by the miniaturisation and solid-state transition of technology, as tech becomes smaller and more efficient with less moving, breakable, parts. Also having a prior interest in electrostatics and high voltage, as it's a field that is as aesthetically pleasing as it is intriguing; these two interests converged when I stumbled upon electro hydrodynamics, particularly ion engines. Having worked on my own mechanical and electronic contraptions beforehand. The idea that an engine powered with high voltage, that has no moving parts, but the propellant itself, could function seems mystical.

The main advantage of ion engines is their high propulsion-to-propellant-mass ratios (and 60-70% efficiency), which allow for more payload to be carried (see **Figure 1**). Together with their low wear-and-tear they are ideal for long-term deep-space missions (Lerner & American Institute of Physics, 2000, p. 17).

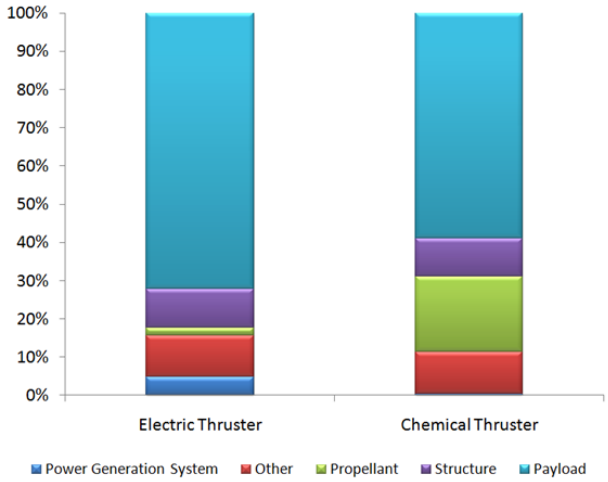

Figure 1: Comparison between electric and chemical propulsion system configurations (Maiorova, Leonov, & Grishko, 2016).

This steered this investigation towards exploring how much thrust could be achieved, and how efficiency behaves around such types of solid-state engines. With a research question of:

To what effect does the electrode separation affect the efficiency of an ion thruster?

Which will be explored through the creation of a theoretical model and analysis of data collected from an experiment conducted on a miniature self-built ion engine.

2 Background Research

2.1 Mechanics Theory

In chemical rockets this is achieved by expanding hot gases through a combustion reaction, which leads to energy losses as the gases do not need to be heated; however due to the high energy density of chemical fuels and their high short-term output, they remain the dominant propulsion method for those applications (Hall & Nasa, 2015).

However, ion thrusters work by ejecting propellant that has been electrically accelerated; providing less, but more reliable thrust with dramatically greater fuel efficiency, because the propellant is minimally heated and can be accelerated to much higher velocities before being ejected (Cain, 2018). This meets the needs for long-term deep space missions.

2.2 Ionic Theory

Ions are simply atoms that have lost or gained one or more electrons, turning them into positively or negatively charged particles.

2.2.1 Ionisation Energy

In order to ionise an atom, energy is required as separating an electron from an atom's positively charged nucleus stores electrical potential energy. The specific amount of energy needed to ionise different atoms is dependent on the strength of the bonds in that substance and the substances effective nuclear charge. Ionisation energy is measured in kJ/mol.

Air is made of 78% di-nitrogen (N_2) molecules, but also contains 21% di-oxygen (O_2), carbon dioxide (CO_2), water (H_2O) and many other impurities (Engineering ToolBox, 2003). This means that the energy required for our model ion thruster to ionise it's propellant is dependent on the composition of the air, something which is controlled in space applications as a specific gas (often Xenon, due to its high atomic mass and inertness as a noble gas) must be stored in a tank to be used as propellant.

Ionisation tends to break bonds in compounds if the removed electron was forming a bond. This can lead to the formation of new substances as the ions recombine into atoms (such as ozone, carbon trioxide, nitrous oxides, etc). Some additional energy may be lost here if it is converted to chemical energy during the formation of a new compound through an endothermic reaction.

2.2.2 Ionisation Mechanisms

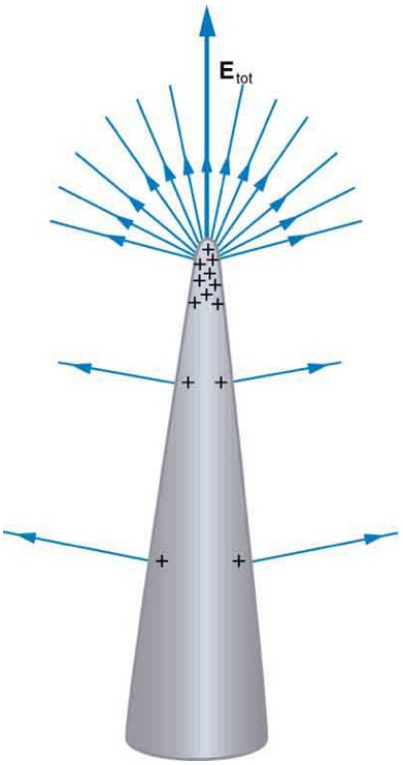

Figure 2: Stronger electric field around sharp edges of conductor. (Lumen Learning, 2017)

Ionisation can happen through several mechanisms. However, for the ion engine design used in this investigation, field desorption through field ionisation is the main mechanism. Field ionisation happens when electrons experience quantum mechanical tunnelling in a high electric field and spontaneously exist outside an atom's orbital valence shell; causing it to lose that electron and become an ion. This effect is greatly amplified by increasing the localised strength of the electric field, which can be done for example by having a conductor with a very sharp tip (as seen in the model ion thruster design) (Lattimer & Schulten, 1989).

Other designs of ion thruster use thermal ionisation (ionisation through the heating of a metal), radio ionisation (ionisation through electromagnetic waves) and other mechanisms.

2.2.3 Townsend Cascade Ionisation

Townsend cascade ionisation or Townsend avalanche is an ionisation phenomenon where a free electron (such as one emitted from the sharp tip of a thruster's anode) is accelerated in an electric field and upon colliding with an atom; the atom becomes a cation by releasing a second electron (see **Figure 3** and **Figure 4**). This emitted electron is then accelerated by the electric field and the

process multiples, hence the name cascade discharge or avalanche discharge (Moyal, 1956).

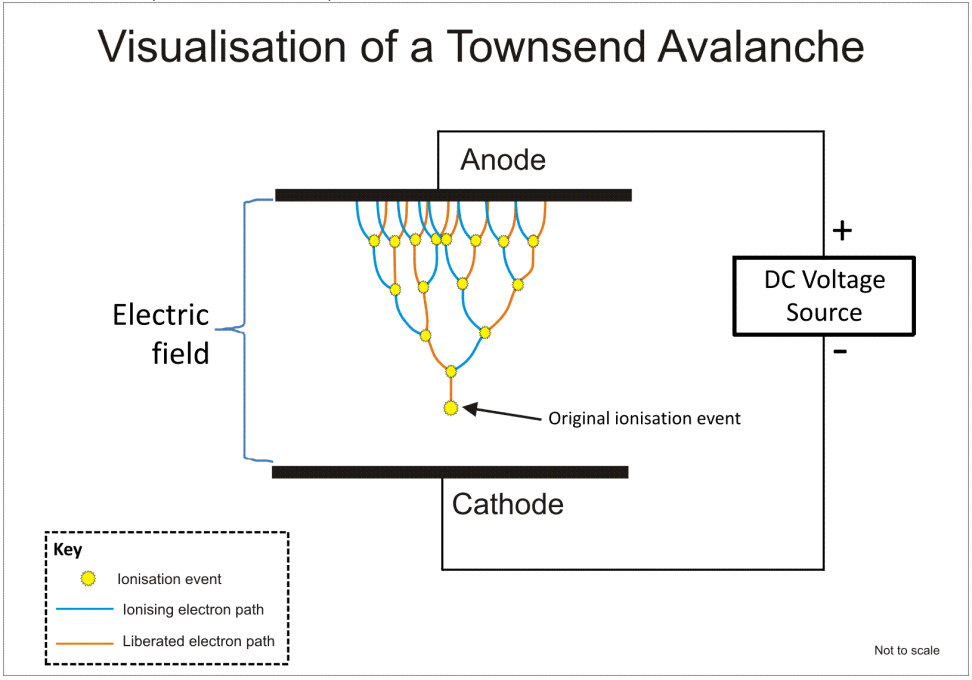

Figure 3: Diagram of cascade ionisation mechanism (Dougsim, 2012).

This phenomenon can be taken advantage of in order to ionise multiple ions per electron emission, as is the case for ion thruster designs with ion chambers which keep the electrons trapped (via magnetic confinement) to maximise collisions that form new ions through Townsend discharge.

2.2.4 Corona Discharge

Corona discharge is another high voltage gas phenomenon where if the strength of an electric field at a conductive surface is stronger than the dielectric strength of the insulating gas (air), charges continuously leak out, causing a purple glow as ions are formed and their electrons transition from excited to relaxed states (illustrated in **Figure 5**). Although this is useful to visually illustrate the strength of the electric field at different points in space (see **Appendix 9.10**), it is an undesired side-effect that decreases efficiency as power is lost with the leaking charges (Fridman & Kennedy, 2004, p. 560)

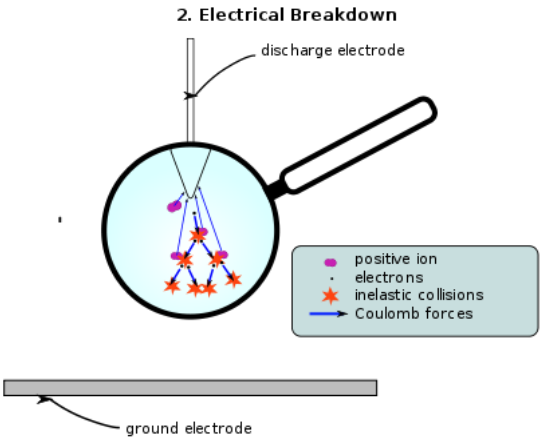

Figure 4: Cascade ionisation initiates corona discharge (Galbrun, 2007).

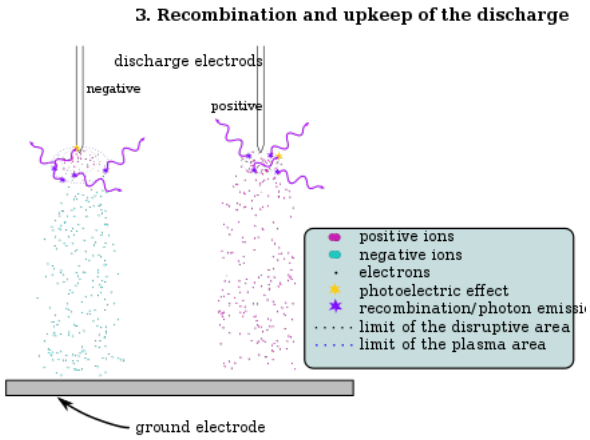

Figure 5: Corona discharge mechanism illustrated (Galbrun, 2007).

2.3 Electrohydrodynamic Theory

Hydrodynamics is the study of fluid mechanics, electrohydrodynamics is the study of fluid mechanics involving electrically charged fluids. It is the key field of research for ion engines and is what allows the design of engines that use no moving parts, but only electricity to make fluids (propellant) move. However, concepts found in hydrodynamics still apply; elastic collisions of gas molecules, Brownian motion, van der Waals forces that cause intermolecular attraction, etc. Importantly for this investigation, since this engine is running in the atmosphere rather than in space; there is air all in the engine which introduces mean free path, which is the average distance a gas molecule travels before colliding with another. Which happens to be 68nm for atmospheric air. This greatly reduces the efficiency of our thruster as the ions only accelerate on average in steps of 68nm at a time before they collide losing energy or changing direction (European Nuclear Society, 2011) (Wikipedia, 2003).

3 Theoretical Modelling

A theoretical model will be created to predict and explore the factors affecting thrust and efficiency, for later experimental comparison.

3.1 Assumptions and Simplifications

In order to build a model to predict the output thrust based on the input power, the following assumptions had to be made in order to simplify the model to a level that is applicable:

1. Every ejected electron transfers all its energy to a single dinitrogen molecule, dinitrogen only.
    a. Assuming no Townsend discharge occurs (see **Townsend Cascade Ionisation**).
2. No energy is lost as light, chemical, sound, heat etc.
    a. Refer to **Ionisation Energy.**
3. Exiting ions do not collide with other atmospheric molecules.
    a. Refer to **Electrohydrodynamic Theory**.
4. Voltage and Current draw are constant. Therefore, resistance of engine is constant.

All these assumptions may provide significant oversight and deviance from experimental results, it does however form a valid hypothesis.

3.2 Predicting Thrust

To predict thrust we need to know the mass and velocity which can be calculated from two factors, the number of ions accelerated, and the amount electrical energy given to each ion.

Potential energy of an electron is one electron volt per volt of potential difference it passes through. Therefore, energy of an electron is equivalent to the potential difference measured in electron volts.

$$E = V \cdot 1e^{-} = V$$

This allows substitution of:

$$E = q \cdot V$$

In order to calculate energy from the voltage of the electrons emitted from the thruster, through the use of units in terms of E, m, and c^2.

Since kinetic energy is known, and can be calculated from mass and velocity, we can then calculate the velocity of the exiting ion:

$$\mathrm{E} = \frac{1}{2}\mathrm{mv}^2$$

Substituting for energy in electron volts:

$$\mathrm{eV} = \frac{1}{2}\mathrm{mv}^2$$

Rearranging for velocity: (Where V=eV=voltage and v=velocity)

$$\mathrm{v}^2 = \frac{2\mathrm{V}}{\mathrm{m}}$$

$$\mathrm{v} = \sqrt{\frac{2\mathrm{V}}{\mathrm{m}}}$$

Mass of particles will be assumed to be dinitrogen molecules (N2). Mass in atomic mass units (amu) multiplied by 9.31×10^8 gives mass in $\mathrm{eV} \cdot \mathrm{c}^{-2}$. Units are gained by rearranging:

$$E = m \cdot c^2$$
$$m = E \cdot c^{-2}$$

This makes resulting velocity in terms of c^2.

$$\mathrm{V} = \sqrt{\frac{2\mathrm{V}}{\mathrm{m}_{\mathrm{N}_2} \cdot 9.31 \times 10^8}}$$

Multiplying by c yields velocity in $\mathrm{m} \cdot \mathrm{s}^{-1}$:

$$\mathrm{v} = 2.99 \times 10^8 \cdot \sqrt{\frac{2\mathrm{V}}{\mathrm{m}_{\mathrm{N}_2} \cdot 9.31 \times 10^8}} \qquad \text{(Eq. 1)}$$

Velocity is acquired, now to calculate force. Momentum is defined as mass multiplied by velocity:

$$\mathrm{p} = \mathrm{mv}$$

Force is mass multiplied by acceleration or change in momentum over time.

$$\mathrm{F} = \mathrm{ma} = \frac{\mathrm{dp}}{\mathrm{dt}}$$

The mass must be multiplied by the number of ions accelerated per second (represented by n), which will be calculated using $\mathrm{C} \cdot \mathrm{s}^{-1}$ from the electrical current used by thruster. Giving the following equation:

$$\mathrm{F} = \mathrm{m}_{\mathrm{N}_2} \cdot \mathrm{v} \cdot \frac{\mathrm{dn}}{\mathrm{dt}}$$

$$\mathrm{F} = \mathrm{m}_{\mathrm{N}_2} \cdot \mathrm{v} \cdot \mathrm{I} \cdot 6.2 \times 10^{18}$$

Converting mass of N_2 to kg:

$$\mathrm{F} = \mathrm{m}_{\mathrm{N}_2} \cdot 1.66 \times 10^{-27} \cdot \mathrm{v} \cdot \mathrm{I} \cdot 6.2 \times 10^{18}$$

Substituting the velocity formula:

$$F = m_{N_2} \cdot 1.66 \times 10^{-27} \cdot 2.99 \times 10^{8} \cdot \sqrt{\frac{2V}{m_{N_2} \cdot 9.31 \times 10^{8}}} \cdot I \cdot 6.2 \times 10^{18}$$

Simplifying:

$$F = m_{N_2} \cdot I \cdot \sqrt{\frac{V}{m_{N_2}}} \cdot \sqrt{\frac{2}{9.31 \times 10^{8}}} \cdot 1.66 \times 10^{-27} \cdot 2.99 \times 10^{8} \cdot 6.2 \times 10^{18}$$

$$F = m_{N_2} \cdot I \cdot \sqrt{\frac{V}{m_{N_2}}} \cdot 1.4263 \times 10^{-4}$$

$$F = I \cdot \sqrt{\frac{V}{m_{N_2}} \cdot {m_{N_2}}^{2}} \cdot 1.4263 \times 10^{-4}$$

$$F = I \cdot \sqrt{\frac{V}{\cancel{m_{N_2}}} \cdot {m_{N_2}}^{\cancel{2}}} \cdot 1.4263 \times 10^{-4}$$

The final result is the formula below:

$$F_{model} = I \cdot \sqrt{V \cdot m_{N_2}} \cdot 1.4263 \times 10^{-4} \qquad \text{(Eq. 2)}$$

Where:

I = Current used by thruster [A]
V = Potential difference across thruster [V]
m_{N_2} = Mass of accelerated particles (N_2) [amu]
F_{model} = Predicted force produced by thruster [N]

The above formula is proven via unit analysis in **Appendix 9.1** (Warn & Stack Exchange, 2018).

This model predicts a linear relationship between the thrust output and the current draw (aka. input power when voltage is fixed); where the slope is determined by the input voltage and mass of ions accelerated. This serves as the hypothesis to this lab; as power input increases, the thrust output will increase linearly.

3.3 Attempt at Predicting Current

An attempt was made to calculate this current using the power supply voltage. The air between the electrodes acts as a resistor, its resistance can be used to calculate the current draw using a known power supply voltage:

$$V = I \cdot R$$

$$I = \frac{V}{R}$$

The resistance of the air gap can be calculated via the resistivity per ion in $\Omega \cdot m^{-1} \cdot n^{-1}$ of air, ρ; the cross section of the gap, A in m^2; and the length of the gap, L in m:

$$R = \frac{n \cdot \rho \cdot L}{A}$$

Substituting, the following formula yields the thruster's current draw:

$$I = \frac{V}{n \cdot \frac{\rho \cdot L}{A}} = \frac{V \cdot A}{n \cdot \rho \cdot L}$$

However, the resistivity of air, ρ, is dependent on the concentration of ions in the gap. It is actually $6 \times 10^{18}\ \Omega \cdot m^{-1}$ per ion which makes problematic to calculate current as resistance changes with the ion concentration which is in itself dependent on many other factors (AlphaLab Inc, 2018). Including but not limited to:

- Number of air particles in the gap.
    - Number of particles limits number of ions able to be created.
- Composition of particles in the gap.
    - Different compounds require different amounts of energy to ionise (differing first ionisation enthalpy)
- Air humidity
    - H_2O is easier to ionise than N_2, with first ionisation enthalpies of $+1218\ kJ \cdot mol^{-1}$ and $+1503\ kJ \cdot mol^{-1}$respectively. Leading to more ions created per energy input when humidity is higher (Truong-Son, 2017) (Chemistry LibreTexts, 2020).
- Number of ions changes as engine starts up.

- Townsend cascade ionisation happens, where atoms eject an electron after ionisation that has enough energy to ionise another atom (see **Townsend Cascade Ionisation**). Leading to a changing number of ions in the gap.

Therefore, attempting to mathematically solve for current by substituting current into ρ yields no useful results as the current value itself is dependent on the current value and can only be experimentally determined, an attempt is made in **Appendix 9.2** nonetheless.

4 Experiment Design

In order to experimentally explore the relationship between the variables used in the formulas above and thrust, a design for an ion thruster was found, based on the simplified original design of R. Goddard's 1917 patent (Beyond NERVA, 2018) (RimstarOrg & Dufresne, 2013). It consists of iron needles for the anode and aluminium tubes for the cathode; the needles' sharp point creates a spot where the electric field is very strong to help ionize the air, the tube cathode which the ions are accelerated towards absorbs the electrons without stopping airflow. A single thruster was made (as seen in **Appendix 9.3**), this was then tripled to provide more thrust to ease measurement. A design was then made for a 3D printed adjustable support structure, that allows for the distance between the electrodes to be varied. This is seen in **Appendix 9.4** with dimensions specified. Final construction is seen in **Appendix 9.5**.

To power the ion thruster, the most readily available high-voltage DC power supply available was a fly-back transformer circuit, like those in CRT televisions. Combined with a Zero Voltage Switching (ZVS) driver board and a 12V 5A switch-mode power supply; this makes a suitable power supply for the thruster.

4.1 Set Up

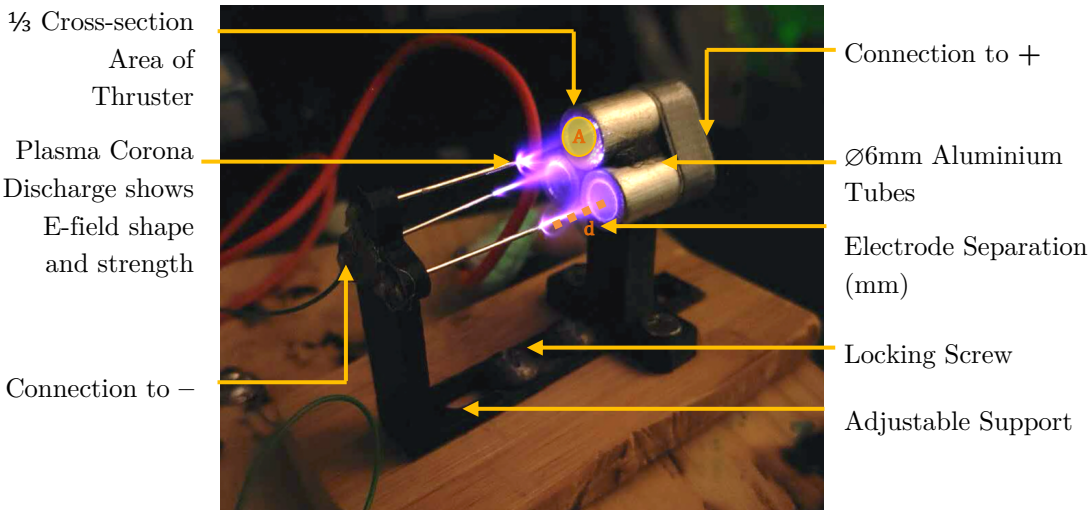

Figure 6: Thruster design labelled

4.1.1 Apparatus

The experimental setup is shown in **Figure 7**, which is according to the schematic in **Figure 8**. Further details are in **Appendix 9.6**.

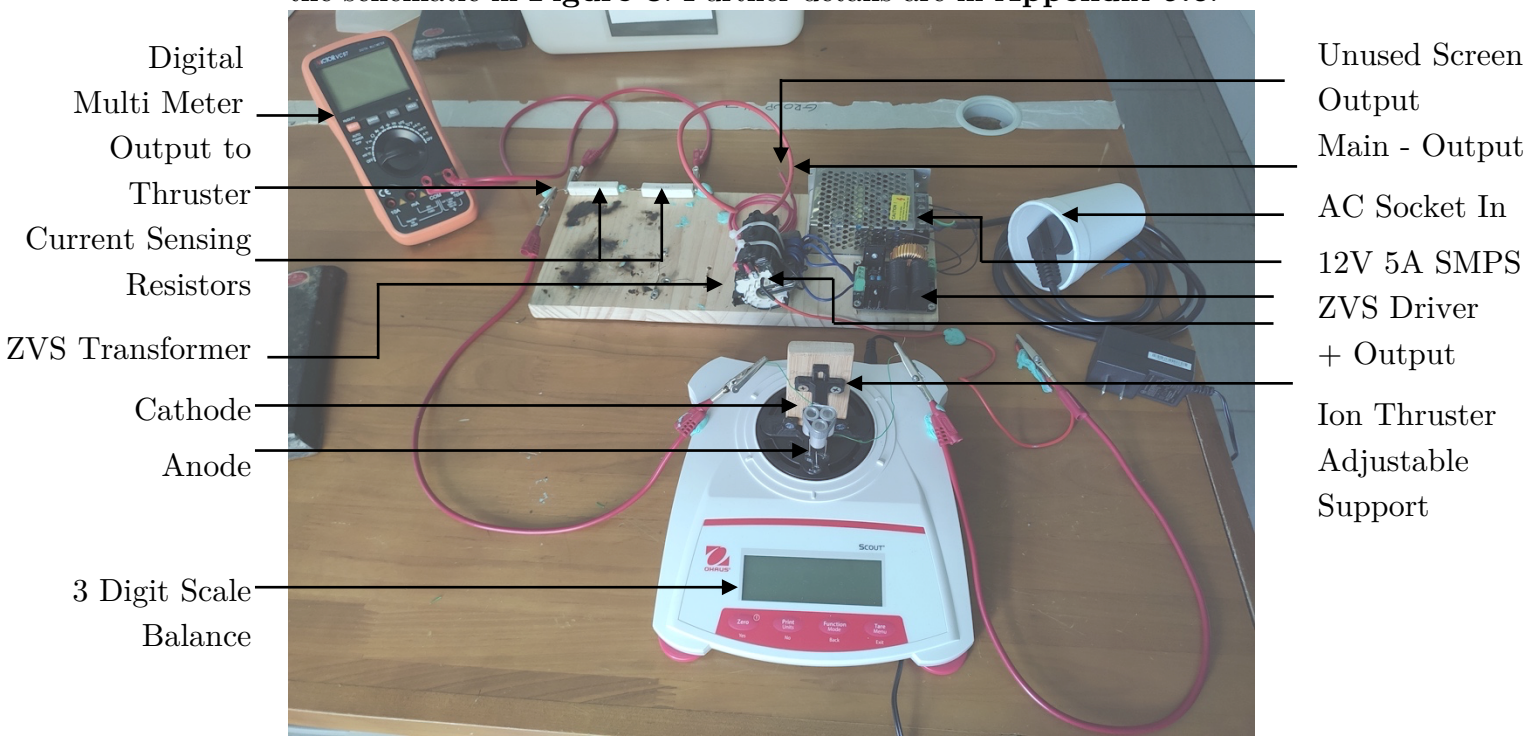

Figure 7: Experiment setup.

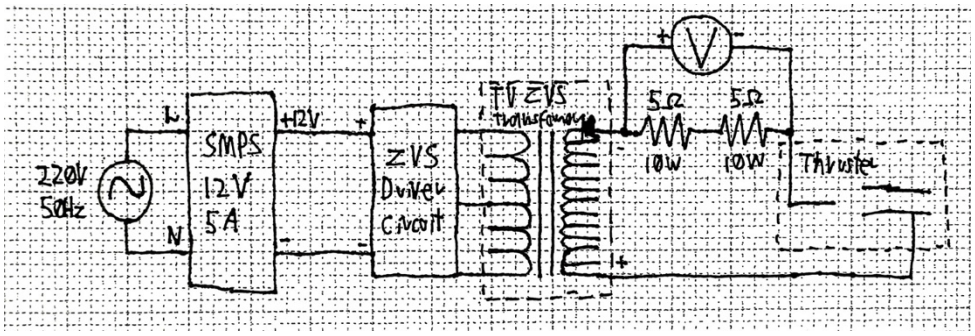

Figure 8: Circuit schematic diagram.

4.1.2 Variables

Category	Variable (units)
Independent Variable	Distance between electrodes (mm) (20mm to 10mm in 1.25mm steps)
Dependent Variable(s)	Thrust produced (g)
	Current draw from power supply (A)
	Output wind speed (ms^{-1})
Controlled/Monitored Variable(s)	Potential Difference of power supply (V) (SMPS keeps constant voltage)
	Humidity and Pressure of air (% and kPa) (trials collected on the same day)
	Shape of electrodes (avoiding electrode melting arc-overs as in **Arc during experiment**)

Table 1: Variables in experiment

All variables were measured with appropriate equipment (e.g. callipers for distance, anemometer for wind speed, etc). However, measuring the thrust and the voltage and current of the high voltage ZVS power supply required a more involved procedure.

The (up to 50kV) high voltage was measured by approaching the output wires and measuring the largest distance in mm (d) where a spark is formed, using the dielectric strength of air ($\kappa_{air} = 3kV \cdot mm^{-1}$ (Hong & Elert, 2000)) the output voltage can be calculated using the formula below:

$$V_{\text{supply}} = d \cdot \kappa_{\text{air}} = d \cdot 3{,}000 \quad \text{(Eq. 3)}$$

Current was measured by placing a 10Ω resistor in series with the ZVS output (as seen in **Figure 8**). Due to the high voltage, two 5Ω 10W high-power ceramic resistors were used in series to ensure sufficient separation. Voltage drop across this resistor was measured in mV with a Digital Multi Meter (DMM), which can be used to calculate current with ohm's law: (I=V/R).

$$I = \frac{V}{R} = \frac{V}{10\Omega}$$

$$I\,[\text{mA}] = \frac{mV}{10} \quad \text{(Eq. 4)}$$

Whereby inputting mV instead of V, returns the current in milliamps.

To calculate the experimental thrust, since the engine is setup to push down on the scale in earth's gravitational field which has a strength of g_0=9.8m · s^{-2}, the weight reading on the scale can easily be converted to force in Newtons (F=ma):

$$F_{\text{experimental}} = m_{\text{scale}} \cdot g_0 \quad \text{(Eq. 5)}$$
$$= m_{\text{scale}} \cdot 9.8$$

4.1.3 Risk Assessment

All the following dangers must be considered before collecting data; lethal risks are present. External supervision is always required; however, the experiment should be carried out individually to reduce risks when other people are involved.

Danger	Source(s)	Precautions
Electrocution	Proximity to high voltage power supply & proximity to anything connected to it. AC mains to SMPS. High voltage will burn, melt and scar skin on contact. May also cause involuntary muscle contraction which can lead to ventricular fibrillation and **death**.	Do not approach or touch anything near the experiment when power is on. Work with a single hand, other behind your back; to avoid risk of current across the chest/heart.
Fire	Short circuit of ZVS output will heat up extremely quickly, melting wires and can cause fire. Short circuit of AC mains will vaporize/explode tips of wires and melt them, can cause fire.	Emergency kill-switch required for mains input, to turn off power without touching arc or wires. Keep calm & turn the power off.
Piercing	Needle tips are sharp. Single strands of wire are sharp.	Don't touch anode needles. Be mindful of wire strands when making electrical connections.
Oxidation	Ionized air produced from the thruster forms an oxidizer, Ozone (O_3). Ozone has a pungent smell and can damage the lungs, causing irritation, coughing or chest pain.	Operate thruster for limited periods of time in an open/ventilated area, to keep ozone concentrations low. Avoid inhaling air exhausted from the thruster.

Table 2: Risk assessment

4.2 Data Collection

4.2.1 Procedure

After assembling the setup (as in **Apparatus**) and measuring the power supply voltage (see **Variables**), the ion thruster's electrode separation was adjusted and locked in place, it was then mounted on the scale and powered on, after collecting each data point the process was repeated across the whole range of electrode separations and for four trials (see **Raw Data**). Air humidity was measured for each trial and high voltage working precautions as well as error precautions were taken.

4.2.2 Raw Data

Distance between electrodes (mm)(±0.01)	Weight (g) (±0.01)				DMM Voltage (mV) (±0.01)				Wind Speed (ms^{-1}) (±0.01)			
	T1	**T2**	**T3**	**T4**	**T1**	**T2**	**T3**	**T4**	**T1**	**T2**	**T3**	**T4**
20.00	0.07	0.06	0.05	0.07	0.17	0.20	0.20	0.17	0.94	0.92	0.97	0.93
18.75	0.10	0.12	0.08	0.09	0.22	0.22	0.23	0.21	0.97	0.93	1.01	0.97
17.50	0.09	0.07	0.10	0.10	0.21	0.22	0.28	0.26	0.99	0.94	1.06	1.02
16.25	0.11	0.10	0.11	0.15	0.29	0.34	0.34	0.31	1.04	1.14	1.08	1.06
15.00	0.12	0.12	0.13	0.12	0.36	0.46	0.44	0.39	1.06	1.20	1.20	1.14
13.75	0.18	0.12	0.16	0.14	0.47	0.48	0.51	0.47	1.26	1.20	1.30	1.20
12.50	0.16	0.17	0.19	0.17	0.57	0.51	0.63	0.67	1.33	1.28	1.33	1.29
11.25	0.20	0.19	0.21	0.19	0.79	0.79	0.90	0.82	1.54	1.60	1.74	1.47
10.00	0.24	0.22	0.24	0.21	0.82	1.07	1.22	1.42	1.62	1.87	1.87	1.74

Table 3: Raw data table.

Arc Distance (±0.01): 10.85mm, Humidity (RH% per trial): 50%, 49%, 48%, 52%.

Qualitative Observations

- A faint purple glow from corona discharge is emitted from the gap.
- The tips of the needles oxidise and turn dark, they seem to lose a bit of their shape; becoming less sharp over time.
- The lock screw did not always hold the slider in place.
- The weight & tension of the wires themselves caused trouble when trying to tare the mass balance, took several tries per run.
- The DMM voltage is a better indicator of separation than mass.

4.3 Data Processing

To begin processing the data, averages of measurements can be taken, and the supply voltage and thruster current can be calculated. All the sample calculations are shown for the values when the distance between electrodes is 20mm as an example.

Sample Calculations

The measurements of weight, voltage and wind speed are averaged using the formula below:

$$\text{Average} = \frac{T_1 + T_2 + T_3 + T_4}{4} \quad \text{(Eq. 6)}$$

$$\text{Average}_{m_{\text{scale}}} = \frac{0.07 + 0.06 + 0.05 + 0.07}{4} = 0.06\ \text{g}$$

$$\text{Average}_{\text{DMM Voltage}} = \frac{0.17 + 0.20 + 0.20 + 0.17}{4} = 0.19\ \text{mV}$$

$$\text{Average}_{v} = \frac{0.94 + 0.92 + 0.97 + 0.93}{4} = 0.94\ \text{m·s}^{-1}$$

Calculating supply voltage using **(Eq. 3)**:

$$V_{\text{supply}} = 10.85 \cdot 3{,}000 = 32{,}550\ \text{V}$$

Calculating current using **(Eq. 4)**:

$$I = \frac{0.19}{10} = 0.019\ \text{mA}$$

Uncertainty Calculations

The uncertainties for the measurements taken over four trials are calculated using the formula below:

$$\Delta\text{Uncertainty} = \frac{T_{\max} - T_{\min}}{2} \quad \text{(Eq. 7)}$$

$$\Delta m_{\text{scale}} = \frac{0.07 - 0.05}{2} = \pm 0.01\ \text{g}$$

$$\Delta \textit{DMM Voltage} = \frac{0.20 - 0.17}{2} = \pm 0.02\ \text{mV}$$

$$\Delta v = \frac{0.97 - 0.92}{2} = \pm 0.03\ \text{m·s}^{-1}$$

The uncertainty for supply voltage is calculated by propagating the uncertainty of the arc distance measurement (in **Table 3**) through the current equation **(Eq. 3)**:

$$\Delta V_{\text{supply}} = 0.01 \cdot 3000 = \pm 30\ \text{V}$$

The uncertainty for current is also calculated by propagating the uncertainty of the DMM Voltage through **(Eq. 4)**:

$$\Delta I = \frac{0.02}{10} = \pm 0.002\ \text{mA}$$

Table 4: Processed data table.

Distance between electrodes (mm)	Average Values						Calculated Values			
	Weight (g)	Unc. (±g)	DMM Voltage (mV)	Unc. (±mV)	Wind Speed (ms^{-1})	Unc. (±ms^{-1})	Supply Voltage (V)	Unc. (±V)	Current (mA)	Unc. (±mA)
20.00	0.06	0.01	0.19	0.02	0.94	0.03			0.019	0.002
18.75	0.10	0.02	0.22	0.01	0.97	0.04			0.022	0.001
17.50	0.09	0.02	0.24	0.04	1.00	0.06			0.024	0.004
16.25	0.12	0.03	0.32	0.03	1.08	0.05			0.032	0.003
15.00	0.12	0.01	0.41	0.05	1.15	0.07	32550	30	0.041	0.005
13.75	0.15	0.03	0.48	0.02	1.24	0.05			0.048	0.002
12.50	0.17	0.02	0.60	0.08	1.31	0.03			0.060	0.008
11.25	0.20	0.01	0.83	0.06	1.59	0.14			0.083	0.006
10.00	0.23	0.02	1.13	0.30	1.78	0.13			0.113	0.030

4.3.1 Applying the Model

To make a comparison, the thrust predicted by the model and the experimental measured thrust is calculated.

Sample Calculations

Calculating predicted thrust using **(Eq. 2)**:

$$\begin{aligned} \mathrm{F_{model}} &= 0.019 \cdot \sqrt{32550 \cdot 28} \cdot 1.4263 \times 10^{-4} \\ &= 2.405\ \mathrm{mN} \end{aligned}$$

Calculating experimental thrust using **(Eq. 5)**:

$$\mathrm{F_{experimental}} = \frac{0.06}{1000} \cdot 9.8 \cdot 1000 = 0.613\ \mathrm{mN}$$

Uncertainty Calculations

Looking at **Equation (**Eq. 2 two variables with uncertainties are used: current (I) which is simply a factor of the rest of the function and voltage (V) which is inside a sub-function; the uncertainty can be calculated by adding the fractional uncertainty of current and the fractional uncertainty of voltage propagated through the sub-function it lays in. In order to convert this sum of fractional uncertainties to absolute uncertainties, it is multiplied by the value whose uncertainty it represents, as described by the formula below:

$$\Delta c = c \cdot \left(\frac{\Delta a}{a} + \frac{\Delta b}{b} \right) \qquad \text{(Eq. 8)}$$

Calculating uncertainty of predicted thrust:

$$\Delta \mathrm{F_{model}} = F_{\mathrm{model}} \cdot \left(\frac{\Delta I}{I} + \frac{\sqrt{\Delta \mathrm{V_{supply}} \cdot 28} \cdot 1.4263 \times 10^{-4}}{\sqrt{\mathrm{V_{supply}} \cdot 28} \cdot 1.4263 \times 10^{-4}} \right)$$

$$= 2.405 \cdot \left(\frac{0.002}{0.019} + \frac{\sqrt{30 \cdot 28} \cdot 1.4263 \times 10^{-4}}{\sqrt{32550 \cdot 28} \cdot 1.4263 \times 10^{-4}} \right)$$
$$= \pm 0.262 \text{ mN}$$

Calculating uncertainty of experimental thrust is done by propagating the uncertainty of the weight measurement through **(Eq. 5)**:

$$\Delta F_{\text{experimental}} = \frac{0.01}{1000} \cdot 9.8 \cdot 1000 = \pm 0.098 \text{ mN}$$

Table 5: Modelled and experimental thrust data table.

Distance between electrodes (mm)	Thrust Modelling			
	Predicted Thrust (mN)	Uncertainty (±mN)	Measured Thrust (mN)	Uncertainty (±mN)
20.00	2.405	0.262	0.613	0.098
18.75	2.860	0.133	0.956	0.196
17.50	3.152	0.523	0.882	0.196
16.25	4.160	0.394	1.152	0.294
15.00	5.362	0.655	1.201	0.098
13.75	6.272	0.266	1.470	0.294
12.50	7.735	1.047	1.691	0.196
11.25	10.724	0.790	1.936	0.098
10.00	14.722	3.913	2.230	0.196

4.3.2 Determining Efficiency

Electrical Efficiency

Thrust efficiency is the amount of force created per unit of power used [N/W], which represents how electrically power efficient the engine is (Petro & Sedwick, 2017, p. 4). It is given by the formula below, where $P_{in}=V \cdot I$:

$$\text{Electrical Efficiency} = \eta_{\text{electrical}} = \frac{F_{\text{experimental}}}{P \cdot I} = \frac{F_{\text{experimental}}}{P_{\text{in}}} \qquad \text{(Eq. 9)}$$

Specific Impulse

However, especially for space applications where mass of a spacecraft is critical; amount of fuel/propellant used per unit of force produced is also important. This is measured by the specific impulse and has the units of seconds; it is the ratio between the force produced as thrust and the equivalent force of the weight (using earth's gravity, g_0=9.8m $\cdot$ s^{-2}) of propellant ejected per second. In order to know the flow rate of the propellant, wind speed must be experimentally measured. (Hall & Nasa, 2015)

$$I_{\text{sp}} = \frac{F_{\text{experimental}}}{\frac{m}{s} \cdot g_0}$$

This can be rewritten in terms of the cross-section area of the thruster (A), the exit velocity of the propellant (v), the density of air (ρ_{air}=1.225 kg $\cdot$ m^{-3}) to obtain the flow rate needed:

$$I_{\text{sp}} = \frac{F_{\text{experimental}}}{A \cdot v \cdot \rho_{air} \cdot g_0} \qquad \text{(Eq. 10)}$$

$$= \frac{F_{\text{experimental}}}{A \cdot v \cdot 1.225 \cdot 9.8}$$

Percent Efficiency

Lastly, the overall percentage efficiency can also be calculated. In order to calculate percentage efficiency, the ratio of power output to power input must be calculated.

Power in can be calculated from the voltage and current draw from the power supply:

$$P = V \cdot I$$

$$P_{\text{in}} = V \cdot I \qquad \text{(Eq. 11)}$$

According to Petro & Sedwick (2017, p. 4), the power output of an ion engine can be calculated using the force produced ($F_{experimental}$), the specific impulse (I_{sp}) and earth's gravitational field strength (g_0=9.8m $\cdot$ s^{-2}), using the formula below:

$$P_{\text{out}} = F_{actual} \cdot I_{sp} \cdot g_0 \qquad \text{(Eq. 12)}$$

With the input and output power calculated, the percent efficiency can then be calculated:

$$\text{Percent Efficiency } = \eta_{\text{percent}} = \frac{P_{\text{out}}}{P_{\text{in}}} \times 100 \qquad \text{(Eq. 13)}$$

Sample Calculations

Calculating power input using **(Eq. 11)**:

$$P_{\text{in}} = 32550 \cdot 0.019 = 0.602 \text{ W}$$

Calculating electrical efficiency using **(Eq. 9)**:

$$\eta_{\text{electrical}} = \frac{0.613}{0.602} = 1.107 \text{ mN·W}^{-1}$$

Calculating specific impulse using **(Eq. 10)**:

$$I_{\text{sp}} = \frac{0.613}{8.48 \cdot 10^{-5} \cdot 0.94 \cdot 1.225 \cdot 9.8} = 0.640 \text{ s}$$

Calculating power output using **(Eq. 12)**:

$$P_{\text{out}} = 0.613 \cdot 0.640 \cdot 9.8 = 0.004 \text{ W}$$

Calculating percent efficiency using **(Eq. 13)**:

$$\eta_{\text{percent}} = \frac{0.004}{0.602} \times 100 = 0.638 \text{ \%}$$

Uncertainty Calculations

For all the values calculated in this efficiency section, their uncertainties can be determined via the fractional uncertainty sum method seen in **(Eq. 8)**.

$$\Delta P_{\text{in}} = 0.602 \cdot \left(\frac{30}{32550} + \frac{0.002}{0.019}\right) = \pm 0.066 \text{ W}$$

$$\Delta P_{\text{out}} = 0.004 \cdot \left(\frac{0.098}{0.613} + \frac{0.119}{0.640}\right) = \pm 0.001 \text{ W}$$

$$\Delta \eta_{\text{percent}} = 0.638 \cdot \left(\frac{0.001}{0.004} + \frac{0.066}{0.602}\right) = \pm 0.256 \text{ \%}$$

$$\Delta \eta_{\text{electrical}} = 1.017 \cdot \left(\frac{0.098}{0.613} + \frac{0.066}{0.602}\right) = \pm 0.274 \text{ mN·W}^{-1}$$

However, specific impulse is calculated from three variables (wind speed, experimental thrust and propagated error in thruster area) therefore it needs the three fractional uncertainties to be added.

$$\Delta I_{\text{sp}} = I_{\text{sp}} \cdot \left(\frac{\Delta F_{\text{experimental}}}{F_{\text{experimental}}} + \frac{\Delta A}{A} + \frac{\Delta v}{v}\right)$$

$$= 0.640 \cdot \left(\frac{0.098}{0.613} + \frac{2.36 \cdot 10^{-10}}{8.48 \cdot 10^{-5}} + \frac{0.03}{0.94}\right) = \pm 0.119 \text{ s}$$

Table 6: Efficiency metrics data table

Distance between electrodes (mm)	Power				Efficiency					
	Power In (W)	Unc. (±W)	Power Out (W)	Unc. (±W)	Percent Efficiency (%)	Unc. (±%)	Electrical Efficiency (mN/W)	Unc. (±mN/W)	Specific Impulse (s)	Unc. (±s)
20.00	0.602	0.066	0.004	0.001	0.638%	0.256%	1.017	0.274	0.640	0.119
18.75	0.716	0.033	0.009	0.004	1.265%	0.630%	1.334	0.336	0.967	0.238
17.50	0.789	0.131	0.007	0.003	0.946%	0.412%	1.117	0.434	0.864	0.196
16.25	1.042	0.099	0.012	0.006	1.134%	0.572%	1.106	0.387	1.047	0.271
15.00	1.343	0.164	0.012	0.002	0.898%	0.151%	0.894	0.182	1.025	0.104
13.75	1.571	0.067	0.017	0.007	1.068%	0.493%	0.936	0.227	1.164	0.280
12.50	1.937	0.262	0.021	0.004	1.086%	0.229%	0.873	0.219	1.270	0.135
11.25	2.685	0.198	0.023	0.004	0.846%	0.169%	0.721	0.090	1.197	0.162
10.00	3.686	0.980	0.027	0.005	0.731%	0.155%	0.605	0.214	1.233	0.168

5 Data Analysis

5.1 Electrode Separation and Power

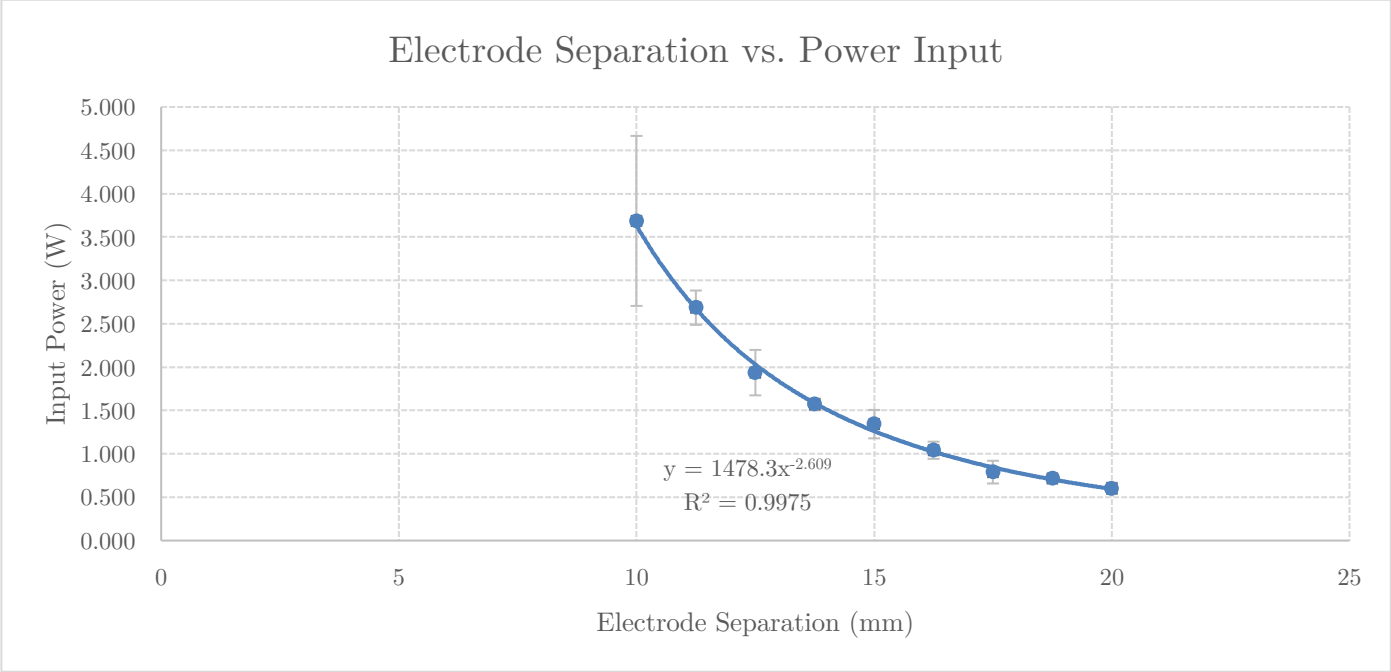

Graph 1

As the electrode separation decreased, the input power draw increased at an increasing rate; forming a power relationship. This is expected because field desorption (as explained in **Ionisation Mechanisms**) increases with field the increasing field strength (V/m) (see matching **Figure 9**) resultant from reducing the separation, leading to more ionisation, more current, and more power. Smaller separation also means more acceleration of ions per distance travelled (less acceleration time, more Coulomb force).

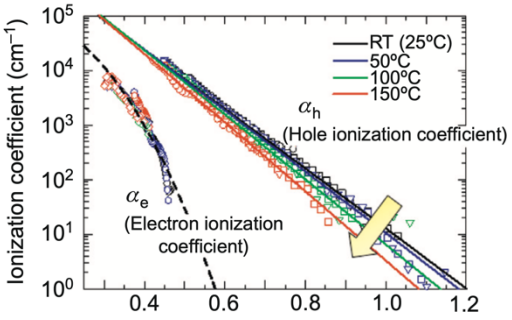

Figure 9: Ionisation coef. vs. Inverse of Electric Field Strength, for Field Ionisation (Kimoto, 2019, p. 29)

The correlation is very strong with a Pearson's coefficient (R^2) of 99.62% and the error bars show precise measurements. This strong relationship made it more significant to compare all other variables against input power rather than electrode separation; this is because input power is a parameter that exists across all ion engine designs, allowing for comparison to existing research.

5.2 Thrust

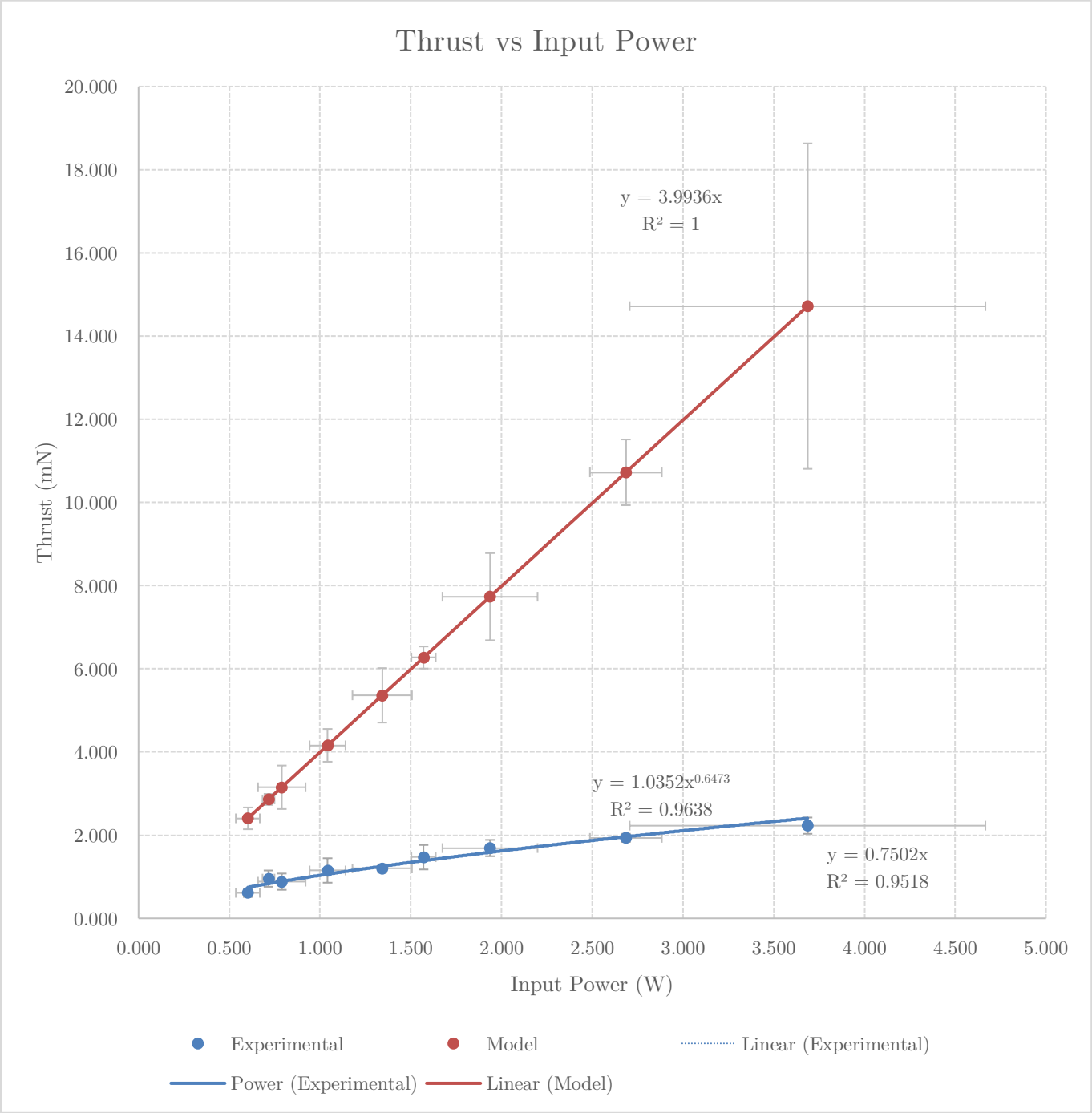

Graph 2

As the power input increases the thrust produced increases. However, the theoretical model predicts a directly proportional linear relationship, with a higher output than the power relationship shown by the experimental thrust.

The significantly smaller output of the experimental thrust can be attributed to losses in the setup, particularly operating in air (where there are molecule collisions). This can be explained by mean free path (as explained in **Electrohydrodynamic Theory**), as ions hit other molecules and loose energy, before accelerating to the maximum velocity available across the whole electric field potential. The non-linearity could be related to air drag, as drag increases proportionally to velocity squared, creating a terminal velocity for ions accelerated in atmospheric air.

The correlation coefficient of 94.18% indicates a very strong trend.

5.3 Efficiency

The percent efficiency was rendered invalid by the limitations of the experimental setup in the atmosphere (shown in **Appendix Graph 6**), however the specific impulse and electrical efficiency remain valid indicators.

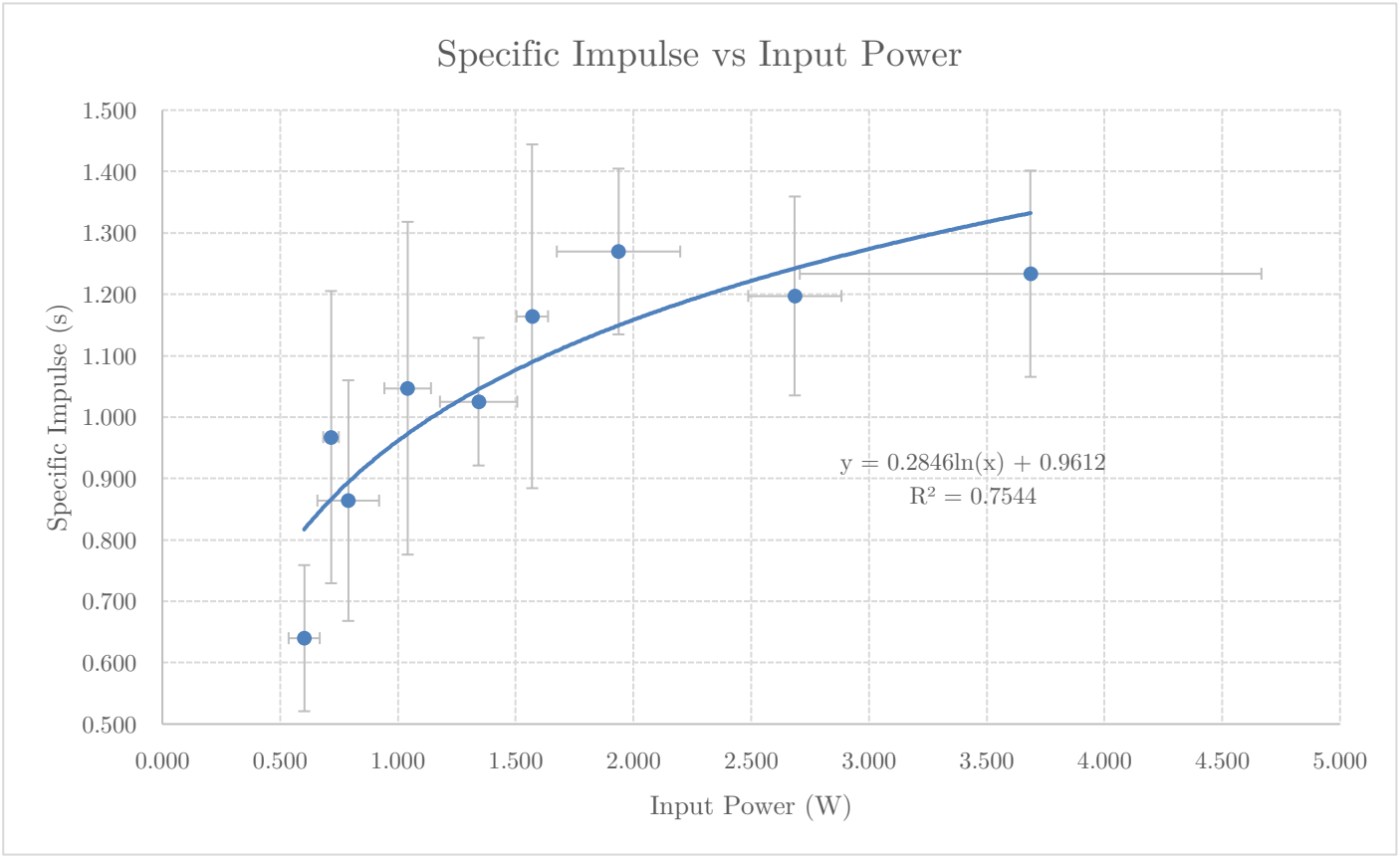

Graph 3

The specific impulse increases logarithmically as input power increases. This suggests that at higher powers, ions are ejected at higher velocities as more thrust is produced per mass ejected, despite the ejection rate increasing (See **Graph 7**).

Once again, mean free path explains this; As ions are able to accelerate to higher velocities when the electrode separation is smaller, and the power input is greater. Additionally, more propellant is used at higher powers as it takes less time for ions to be ejected. This trend would suggest higher efficiency at higher input powers. The correlation coefficient of 75.44% denotes a strong trend.

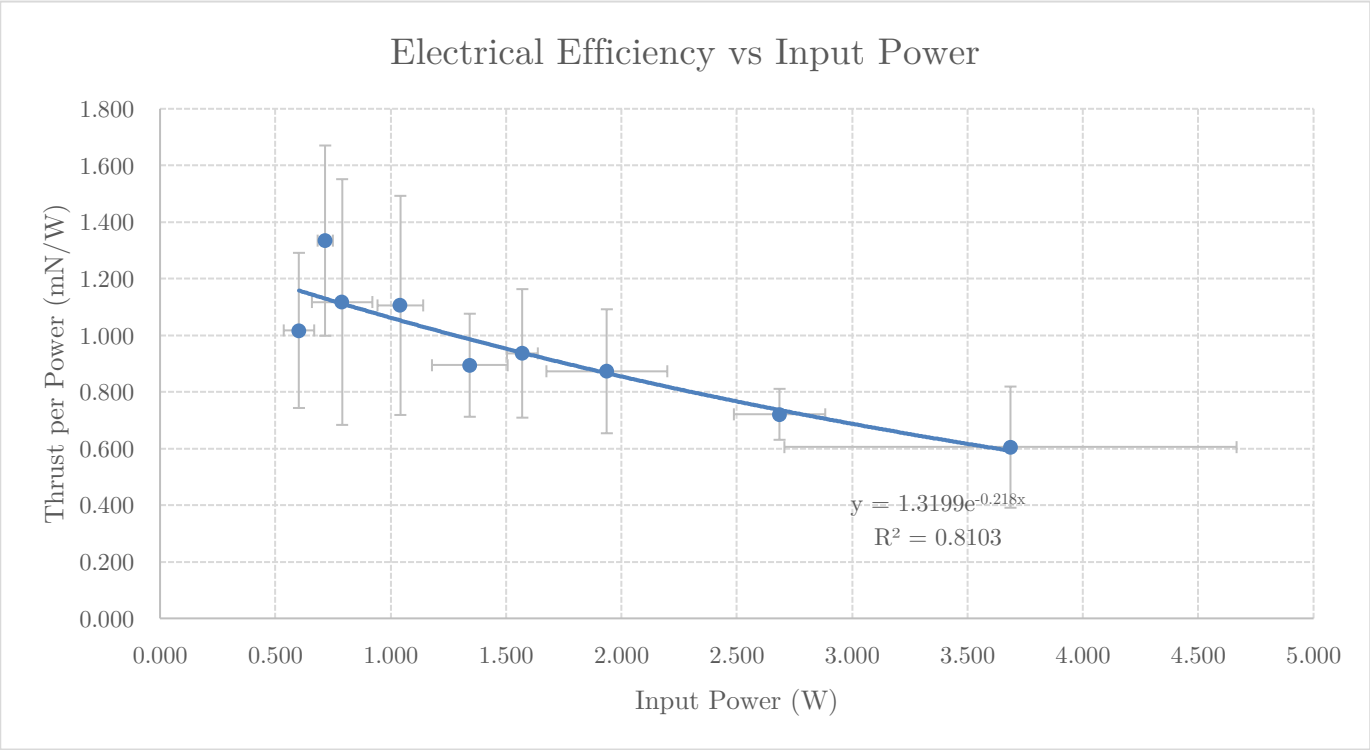

Graph 4

As the input power increases, the electrical efficiency decreases exponentially (with a decreasing rate); this is an inverse relationship to the one experienced by specific impulse. This means that at lower powers, the engine creates more thrust per power input than at higher powers. The R^2 value of 87.44% denotes a strong correlation. This suggests inefficiency at higher powers however, both propellant (impulse) efficiency and electrical efficiency must be considered simultaneously.

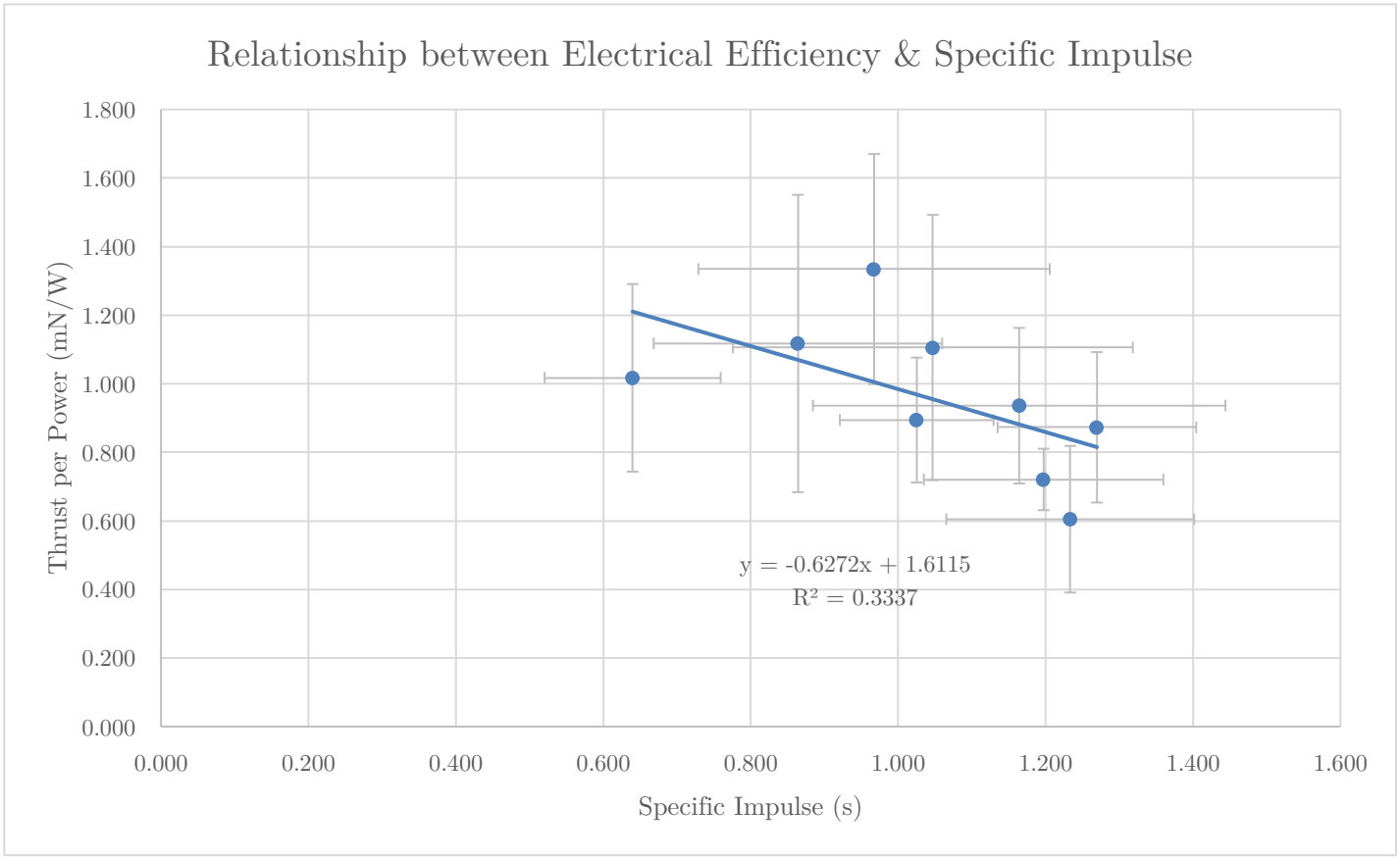

Graph 5

The negative linear relationship between thrust-per-power and specific impulse clearly summarises the efficiency trade-off presented by the data. When specific impulse is higher, less propellant is used per thrust generated. However, this is due to more electrical energy being used to accelerate the propellant faster, in-turn decreasing the electrical efficiency (thrust-per-power). At lower input powers, the engine prefers to use more propellant per thrust (low specific impulse) but accelerate the propellant less (high electrical efficiency). This is described by the equation below in terms of conservation of energy:

$$\mathrm{E} = \frac{V \cdot I}{t} = \mathrm{KE} = \frac{1}{2} \cdot m \cdot v^2 \qquad \text{(Eq. 14)}$$

However, the engine's preference of mass vs. velocity trade-off could be a side-effect of the increased flow-rate at higher powers caused by the free mean path and the smaller electrode separation.
The R^2 value of 33.37% is less than optimal, however still indicative of a valid trend.

6 Conclusion

The outcome of the investigation is that the electrode separation of an ion thruster greatly affects the efficiency of an ion thruster; by changing multiple parameters, the efficiency is skewed towards being propellant-efficient or electrically efficient.

Reducing the separation alters two main aspects: the number of ions generated increases as the electric field strength increases which enhances field ionisation through desorption, and the exit velocity of the ions increases as a stronger electric field accelerates ions faster over the mean free path distance (of which there are also less of across the field thanks to the smaller separation), helping to reduce the losses due to atmospheric collisions.

At smaller separations, the increased ionisation rate increases the propellant flow rate which causes more electrical power to be drawn as the the ions accelerate to a higher velocity in the presence of a stronger electric field; increasing specific impulse. At larger separations, the weaker electric field causes the ions to be accelerated less over the mean free path, combined with the decreased flow rate, which leads to more propellant being accelerated less; increasing thrust-per-power.

6.1 Strengths & Limitations

Various strengths and limitations are identified throughout the investigation. The main issue is testing the thruster in an atmosphere, which introduced losses that greatly reduced and invalidated its total efficiency (by an order of magnitude) and changed its behaviour by enforcing a small mean free path. Other issues surround the limitations of complexity that cannot be modelled (often arising from the atmospheric complication), such as the multiple atmospheric gases, energy losses to light, heat, etc, and energy loses to dispersion to atmospheric molecules.

The main strength of this investigation is that it managed to provide valid trends coherent with external experimental research (with confident R^2 values), despite its physical inaccuracies. For instance;

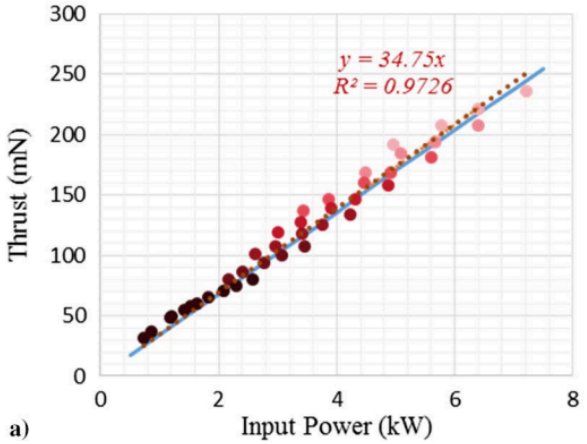

Figure 10: Plot of thrust versus input power for DC ion engines (Petro & Sedwick, 2017, p. 6).

- **Graph 2**'s theoretical model matches **Figure 10**'s experimental research data. The relationship between thrust and input power is directly proportional experimentally when the engine is in a vacuum rather than the atmosphere.

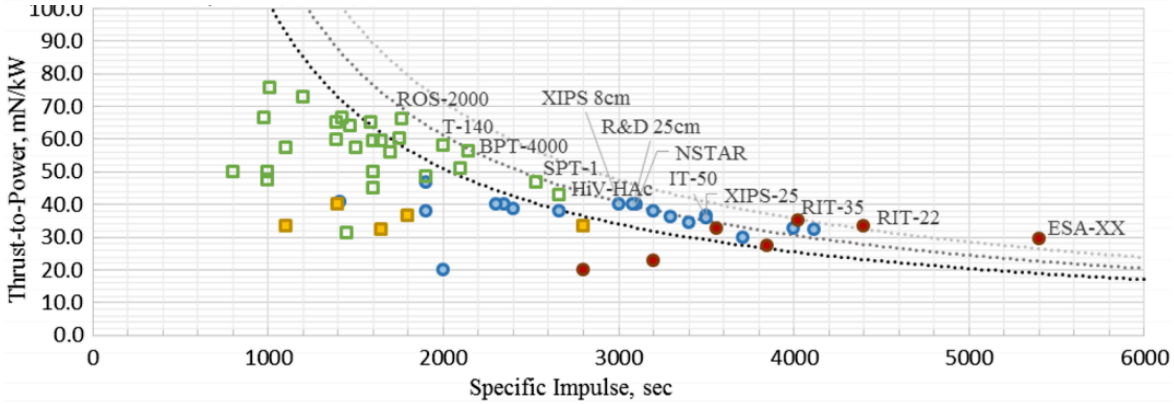

Figure 11: Plot of thrust-to-power versus specific impulse for different engine models (Petro & Sedwick, 2017, p. 9).

- The trade-off relationship found between specific impulse and thrust-per-power (shown in **Graph 5**) holds true for real engines. Different designs are optimised for prioritising one efficiency type over the other (shown in **Figure 11**).

6.2 Extensions

The straight-forward extensions to make fix the physical inaccuracies of the current experiment: running in atmosphere, not having an ion-containment chamber in the design, and not running with controlled propellant.

More extensions can be made to explore additional variables such as the impact of: air humidity (see **Graph 8**), propellant type, voltage, etc.

7 Evaluation

7.1 Reliability of Collected Data

Table 7: Percentage uncertainty for all variables, colour shaded.

Distance between electrodes (mm)	Percentage Uncertainty (%)											
	Weight	DMM Voltage	Wind Speed	Supply Voltage	Current	Predicted Thrust	Measured Thrust	Power In	Power Out	Percent Efficiency	Electrical Efficiency	Specific Impulse
20	16.7%	10.5%	3.2%	0.1%	10.5%	10.9%	16.0%	11.0%	25.0%	40.1%	26.9%	18.6%
18.75	20.0%	4.5%	4.1%		4.5%	4.7%	20.5%	4.6%	44.4%	49.8%	25.2%	24.6%
17.5	22.2%	16.7%	6.0%		16.7%	16.6%	22.2%	16.6%	42.9%	43.6%	38.9%	22.7%
16.25	25.0%	9.4%	4.6%		9.4%	9.5%	25.5%	9.5%	50.0%	50.4%	35.0%	25.9%
15	8.3%	12.2%	6.1%		12.2%	12.2%	8.2%	12.2%	16.7%	16.8%	20.4%	10.1%
13.75	20.0%	4.2%	4.0%		4.2%	4.2%	20.0%	4.3%	41.2%	46.2%	24.3%	24.1%
12.5	11.8%	13.3%	2.3%		13.3%	13.5%	11.6%	13.5%	19.0%	21.1%	25.1%	10.6%
11.25	5.0%	7.2%	8.8%		7.2%	7.4%	5.1%	7.4%	17.4%	20.0%	12.5%	13.5%
10	8.7%	26.5%	7.3%		26.5%	26.6%	8.8%	26.6%	18.5%	21.2%	35.4%	13.6%

Different variables are derived from various measurements, having differing percentage uncertainties (see **Table 7**). The data was sufficiently reliable to allow valid conclusions with strong correlations (as in **Data Analysis**).

7.2 Sources of Error

Sources of error are identified throughout **Theoretical Modelling** and **Data Analysis**, below is a summary of the sources and possible improvements.

Table 8: Sources of error categorized into areas of origin and type of error.

Area	Error / Impact on Data	Type	Improvement
Equipment	Scale needs to be tared multiple times → The weight of the wires on the scale changes too easily and frequently. Changes during data collection may have modified the weight readings. Increasing range and decreasing reliability. → Inconvenience caused by multiple tarings increases chances of operator error, which can increase amounts of outliers or need for re-trials.	Systemic Gross	Lighter wires could minimise their weight on the scale. Mounting the engine non-vertically would eliminate the weight and taring issue, although requiring more precise and complex measurement equipment
	Over time the sharp electrode tips became dull. → Duller electrodes create weaker electric fields at the tips. Decreasing the validity of the collected data as the electric field strength is now not perfectly constant across trials. → Arcing forms a hot plasma that melts the tips, needing replacement of the anode.	Systemic	A metal that is more resistant to corrosion via ionisation could be used, or electrodes could be swapped for new ones between trials.
Setup	Set screw mechanism hard to lock in place. → Loose electrodes might have shifted when being mounted back on the scale, making a significant difference as the distance increments are so small (1.25mm). Decreasing reliability as this causes more distance variations between trials.	Random	A better locking mechanism could be designed. Or even a motorised / computer controlled sliding electrode.
	Since the high ZVS output voltage cannot be measured directly or continuously, it may have changed with current draw; instead of remaining constant. → This would have changed the calculated power input, decreasing the validity of the collected data as the voltage was different than the experimental value.	Systemic	A high-voltage probe would solve the issue of being able to measure the ZVS output. An oscilloscope could be used to monitor the voltage change over time.

Method	Temperature and air humidity are both factors that affect the number of ions created via field adsorption. → These monitored variables can't be controlled, only measured. Therefore, they inevitably affect the validity of the experiment. As ambient humidity and temperature don't tend to change rapidly, they are approximately the same for each day of trial collected and can therefore be considered in between systemic error and random error.	Systemic / Random	Conducting the experiment in a vacuum like intended would eliminate all these issues related to the inconsistencies of the atmosphere.
	Many variables are measured in order to calculate single parameters, this adds measurement uncertainties and reduces the validity of calculated parameters. Having many variables also makes it more difficult to isolate causes behind phenomena.	-	Unavoidable when modelling complex systems that take into account many variables.

8 References List

AlphaLab Inc. (2018, March 30). About air ions. Retrieved May 14, 2020, from https://www.alphalabinc.com/about-air-ions/

Beyond NERVA. (2018, October 24). Electric propulsion Part 2: Electrostatic propulsion. Retrieved November 3, 2020, from https://beyondnerva.com/2018/10/24/electric-propulsion-part-2-electrostatic-propulsion/

Cain, F. (2018, May 15). *How Do Ion Engines Work? The Most Efficient Propulsion System Out There* [Video]. Retrieved May 14, 2020, from https://www.youtube.com/watch?v=6H0qsqZjLW0

Chemistry LibreTexts. (2020, August 15). Ionization energies of diatomic molecule. Retrieved November 22, 2020, from https://chem.libretexts.org/Bookshelves/Physical_and_Theoretical_Chemistry_Textbook_Maps/Supplemental_Modules_(Physical_and_Theoretical_Chemistry)/Atomic_Theory/Ionization_Energies_of_Diatomic_Molecule

Croatian, J. (2014, April 1). *Corona Discharge Collage* [Photograph Collage]. Retrieved May 14, 2020, from https://en.wikipedia.org/wiki/File:Corona_Discharge_Collage.jpg

Dougsim. (2012, October 22). *Visualisation of a Townsend Avalanche* [Diagram]. Retrieved November 3, 2020, from https://commons.wikimedia.org/wiki/File:Electron_avalanche.gif

Dudzinski, L., & Anderson, D. J. (2014, January). Solar Electric Propulsion (SEP) Systems for SMD Mission Needs. Retrieved November 3, 2020, from https://www.lpi.usra.edu/opag/meetings/jan2014/presentations/24_anderson.pdf

Engineering ToolBox. (2003). Air - Composition and molecular weight. Retrieved November 27, 2020, from https://www.engineeringtoolbox.com/air-composition-d_212.html

European Nuclear Society. (2011, November 5). Mean free path. Retrieved November 27, 2020, from https://web.archive.org/web/20111105115303/www.euronuclear.org/info/encyclopedia/m/mean-fee-path.htm

Fridman, A., & Kennedy, L. A. (2004). *Plasma physics and engineering*. Retrieved May 05, 2020, from CRC Press.

Galbrun, E. (2007, October 7). *Corona discharge upkeep* [Diagram]. Retrieved November 27, 2020, from https://en.wikipedia.org/wiki/File:Corona_discharge_upkeep.svg

Galbrun, E. (2007, October 7). *Corona electrical breakdown* [Diagram]. Retrieved November 27, 2020, from https://en.wikipedia.org/wiki/File:Corona_electrical_breakdown.svg

Hall, N., & Nasa. (2015, May 5). General thrust equation. Retrieved November 3, 2020, from https://www.grc.nasa.gov/www/k-12/airplane/thrsteq.html

Hall, N., & Nasa. (2015, May 5). Specific impulse. Retrieved November 3, 2020, from https://www.grc.nasa.gov/www/k-12/airplane/specimp.html

Hong, A., & Elert, G. (2000). Dielectric strength of air. Retrieved November 23, 2020, from https://hypertextbook.com/facts/2000/AliceHong.shtml

IonTrading. (n.d.). Theory of air ion. Retrieved May 14, 2020, from https://www.n-ion.com/e/theory.html

Keystone Science. (2017, July 19). *How to make an Ion Thruster* [Video]. Retrieved December 18, 2019, from https://www.youtube.com/watch?v=_TYvUdaLjRA

Kimoto, T. (2019). SiC material properties. *Wide Bandgap Semiconductor Power Devices*, 21-42. Retrieved November 23, 2020, from doi:10.1016/b978-0-08-102306-8.00002-2

Kreosan. (2018, January 10). *I've assembled an Ion Thrust Engine at home* [Video]. Retrieved December 18, 2019, from https://www.youtube.com/watch?v=5HL1tiWEDls

Lattimer, R. P., & Schulten, H. (1989). Field ionization and field desorption mass spectrometry: Past, present, and future. *Analytical Chemistry*, *61*(21), 1201A-1215A. Retrieved November 3, 2020, from doi:10.1021/ac00196a721

Lerner, E. J., & American Institute of Physics. (2000, October). Plasma Propulsion in Space. *The Industrial Physicist*, *6*, 16-19. Retrieved May 14, from https://web.archive.org/web/20070316160623/http://www.aip.org/tip/INPHFA/vol-6/iss-5/p16.pdf

Lumen Learning. (2017). Conductors and electric fields in static equilibrium | Physics. Retrieved November 27, 2020, from https://courses.lumenlearning.com/physics/chapter/18-7-conductors-and-electric-fields-in-static-equilibrium/

Maiorova, V., Leonov, V., & Grishko, D. (2016). Analysis of approaches to the near-earth orbit cleanup from space debris of the size Below10 CM. *Aerospace Scientific Journal*, *16*(01). Retrieved November 3, 2020, from doi:10.7463/aersp.0116.0833914

Massachusetts Institute of Technology: OpenCouseWare. (2015, March). *16.522 Space Propulsion: Electrostatic Thrusters (Kaufman Ion Engines)* [PDF Document]. Retrieved May 14, 2020, from https://ocw.mit.edu/courses/aeronautics-and-astronautics/16-522-space-propulsion-spring-2015/lecture-notes/MIT16_522S15_Lecture10-11.pdf

Moyal, J. (1956). Theory of the ionization Cascade. *Nuclear Physics*, *1*(8), 180-195. Retrieved November 27, 2020, from doi:10.1016/s0029-5582(56)80025-4

NA. (n.d.). Thruster Principles. Retrieved May 14, 2020, from https://descanso.jpl.nasa.gov/SciTechBook/series1/Goebel_02_Chap2_thruster.pdf

Patterson, M., Glenn Research Center, & National Aeronautics and Space Administration. (2008, December 22). GRC - Ion Propulsion Overview. Retrieved March 11, 2020, from https://www.grc.nasa.gov/www/ion/overview/overview.htm

Patterson, M., & Nasa. (2015, August 18). Ion propulsion. Retrieved December 18, 2019, from https://www.nasa.gov/centers/glenn/about/fs21grc.html

Patterson, M., & National Aeronautics and Space Administration. (2016, January 11). Ion Propulsion. Retrieved March 2, 2020, from https://www.nasa.gov/centers/glenn/about/fs21grc.html

Petro, E. M., & Sedwick, R. J. (2017). Survey of moderate-power electric propulsion systems. *Journal of Spacecraft and Rockets*, *54*(3), 529-541. Retrieved May 14, 2020, from doi:10.2514/1.a33647

RimstarOrg, & Dufresne, S. (2013, December 15). *How Ion Propulsion, Lifters and Ionocrafts Work* [Video]. Retrieved December 18, 2019, from https://www.youtube.com/watch?v=01F8V5IhB5k

Seeker. (2019, January 13). *The X3 Ion Thruster Is Here, This Is How It'll Get Us to Mars* [Video]. Retrieved May 14, 2020, from https://www.youtube.com/watch?v=CiWb44VRZGo

Tracy, N. (2013, April 24). *Introduction to Ion Thrusters* [Video]. Retrieved December 18, 2019, from https://www.youtube.com/watch?v=grU8g9jnS4w&ab_channel=NateTracy

Truong-Son, N. (2017, July 29). What is the ionization energy of water in kJ/mol? Is it endothermic or exothermic reaction? Retrieved November 22, 2020, from https://socratic.org/questions/what-is-the-ionization-energy-of-water-in-kj-mol-is-it-endothermic-or-exothermic

Uhoh. (2018, March 5). Troubleshooting a DIY ion thruster. Retrieved May 14, 2020, from https://space.stackexchange.com/questions/25811/troubleshooting-a-diy-ion-thruster?rq=1

User17622. (2017, February 3). Why are ion thrusters so energy hungry? Retrieved November 3, 2020, from https://space.stackexchange.com/questions/20017/why-are-ion-thrusters-so-energy-hungry

VideoFromSpace. (2013, September 10). *New NASA Ion Thruster To Propel Spacecraft To 90,000 MPH | Video* [Video]. Retrieved May 14, 2020, from https://www.youtube.com/watch?v=HcEc7dnRppw

Wang, B., & NextBigFuture. (2017, April 7). Magnetoplasmadynamic thrusters can have hundreds of times the thrust of ion propulsion for space application. Retrieved November 3, 2020, from https://www.nextbigfuture.com/2016/04/magnetoplasmadynamic-thrusters-can-have.html

Warn, C. (2018, April 4). Ion thruster thrust calculation problem. Retrieved May 14, 2020, from https://space.stackexchange.com/questions/26449/ion-thruster-thrust-calculation-problem

Warn, C., & Stack Exchange. (2018, April 4). Ion thruster thrust calculation problem. Retrieved May 14, 2020, from https://space.stackexchange.com/questions/26449/ion-thruster-thrust-calculation-problem

Wikipedia. (2001, July 26). Electronvolt. Retrieved May 14, 2020, from https://en.wikipedia.org/wiki/Electronvolt

Wikipedia. (2002, February 5). Ion thruster. Retrieved December 18, 2019, from https://en.wikipedia.org/wiki/Ion_thruster

Wikipedia. (2003, September 14). Corona discharge. Retrieved November 27, 2020, from https://en.wikipedia.org/wiki/Corona_discharge

Wikipedia. (2003, January 17). Mean free path. Retrieved November 27, 2020, from https://en.wikipedia.org/wiki/Mean_free_path

Wikipedia. (2004, March 25). Air ioniser. Retrieved May 14, 2020, from https://en.wikipedia.org/wiki/Air_ioniser

Wikipedia. (2005, May 4). Electrostatic precipitator. Retrieved May 14, 2020, from https://en.wikipedia.org/wiki/Electrostatic_precipitator#Modern_industrial_electrostatic_precipitators

Wikipedia. (2005, February 26). Electrical mobility. Retrieved May 14, 2020, from https://en.wikipedia.org/wiki/Electrical_mobility

Wikipedia. (2006, December 7). Field desorption. Retrieved November 27, 2020, from https://en.wikipedia.org/wiki/Field_desorption

Wikipedia. (2006, December 7). Field desorption. Retrieved November 27, 2020, from https://en.wikipedia.org/wiki/Field_desorption

Wikipedia. (2006, September 9). Townsend discharge. Retrieved November 27, 2020, from https://en.wikipedia.org/wiki/Townsend_discharge

Wikipedia. (2017, June 7). Hollow cathode effect. Retrieved December 18, 2019, from https://en.wikipedia.org/wiki/Hollow_cathode_effect

9 Appendix

9.1 Proving thrust model with unit analysis

Through unit analysis, the above formula can be proved.

For simplification the formula is broken into sections and variables are then replaced with units. Therefore:

$$F = m_{N_2} \cdot 1.66 \times 10^{-27} \cdot 2.99 \times 10^{8} \cdot \sqrt{\frac{2V}{m_{N_2} \cdot 9.31 \times 10^{8}}} \cdot I \cdot 6.2 \times 10^{18}$$

Becomes:

$$N = (amu \cdot \#)(kg) \cdot \left(c \cdot \sqrt{\frac{V\,(eV)}{amu \cdot \#\,(eV \cdot c^2)}}\,(c^{-1}) \right)(m \cdot s^{-1}) \cdot \left(\frac{C}{S} \cdot C\right)(s^{-1})$$

Each section can then be simplified:

Section	Explanation	Resulting Unit
$amu \cdot \#$	Multiplication of amu by kg conversion factor (1.66×10^{-27}).	kg
V	$V \cdot 1e^{-} = eV$	eV
$amu \cdot \#$	Multiplication of amu by $eV \cdot c^2$ conversion factor (9.31×10^{8}).	$eV \cdot c^2$
$\frac{eV}{eV \cdot c^2}$	$\frac{\cancel{eV}}{\cancel{eV} \cdot c^2} = c^{-2}$	c^{-2}
$\sqrt{c^{-2}}$	Square root removes exponent	c^{-1}
$c^{-1} \cdot c$	c is in $m \cdot s^{-1}$, unit multiplication removes value of c	$m \cdot s^{-1}$
$\frac{C}{s} \cdot C$	Coulomb is a quantity; unit multiplication removes value of C	s^{-1}
$kg \cdot m \cdot s^{-1} \cdot s^{-1}$	$= kg \cdot m \cdot s^{-2} = m \cdot a = F$	N

Table 9: Unit analysis breakdown for thrust modelling formula.

9.2 Attempting to solve for thruster current draw

Attempt at obtaining ion count from current:

$$I = \frac{V \cdot A}{\rho \cdot \left(I \cdot 6.2 \times 10^{18}\right) \cdot L}$$

Solving for I by substituting real values:

$$\begin{aligned} &\mathrm{V} = 36{,}000\mathrm{V} \\ &\mathrm{A} = 3 \text{ circles with radius of } 3\mathrm{mm} \\ &\mathrm{L} = 12\mathrm{mm} \end{aligned}$$

$$I = \frac{36000 \cdot (3 \cdot \pi \cdot 0.003^2)}{6 \times 10^{18} \cdot \left(I \cdot 6.2 \times 10^{18}\right) \cdot 0.012}$$

$$I = \frac{3.0536}{\mathrm{I} \cdot 4.464 \times 10^{35}}$$

$$I \cdot 4.464 \times 10^{35} = \frac{3.0536}{\mathrm{I} \cdot 4.464 \times 10^{35}} \cdot 4.464 \times 10^{35}$$

$$I \cdot 4.464 \times 10^{35} = \frac{3.0536}{\cancel{\mathrm{I} \cdot 4.464 \times 10^{35}}} \cdot \cancel{4.464 \times 10^{35}}$$

$$I \cdot 4.464 \times 10^{35} \cdot \mathrm{I} = \frac{3.0536}{\mathrm{I}} \cdot \mathrm{I}$$

$$I^2 \cdot 4.464 \times 10^{35} = \frac{3.0536}{\cancel{\mathrm{I}}} \cdot \cancel{\mathrm{I}}$$

$$I^2 \cdot 4.464 \times 10^{35} = 3.0536$$

$$I^2 = \frac{3.0536}{4.464 \times 10^{35}}$$

$$I = \sqrt{\frac{3.0536}{4.464 \times 10^{35}}}$$

$$I = 2.6154 \times 10^{-18}\ A$$

$$n = I \cdot 6.2 \times 10^{18}$$

$$n = 2.6154 \times 10^{-18} \cdot 6.2 \times 10^{18}$$

$$n = 16.2155\ ions$$

The result returns the current when there only ~16 ions in the air gap, which is completely invalid. A much more complex approach would be needed to calculate the current, which is out of the scope of this extended essay.

Therefore, current must be a measured parameter rather than a calculated one when applying the model.

9.3 Early Prototype Thruster

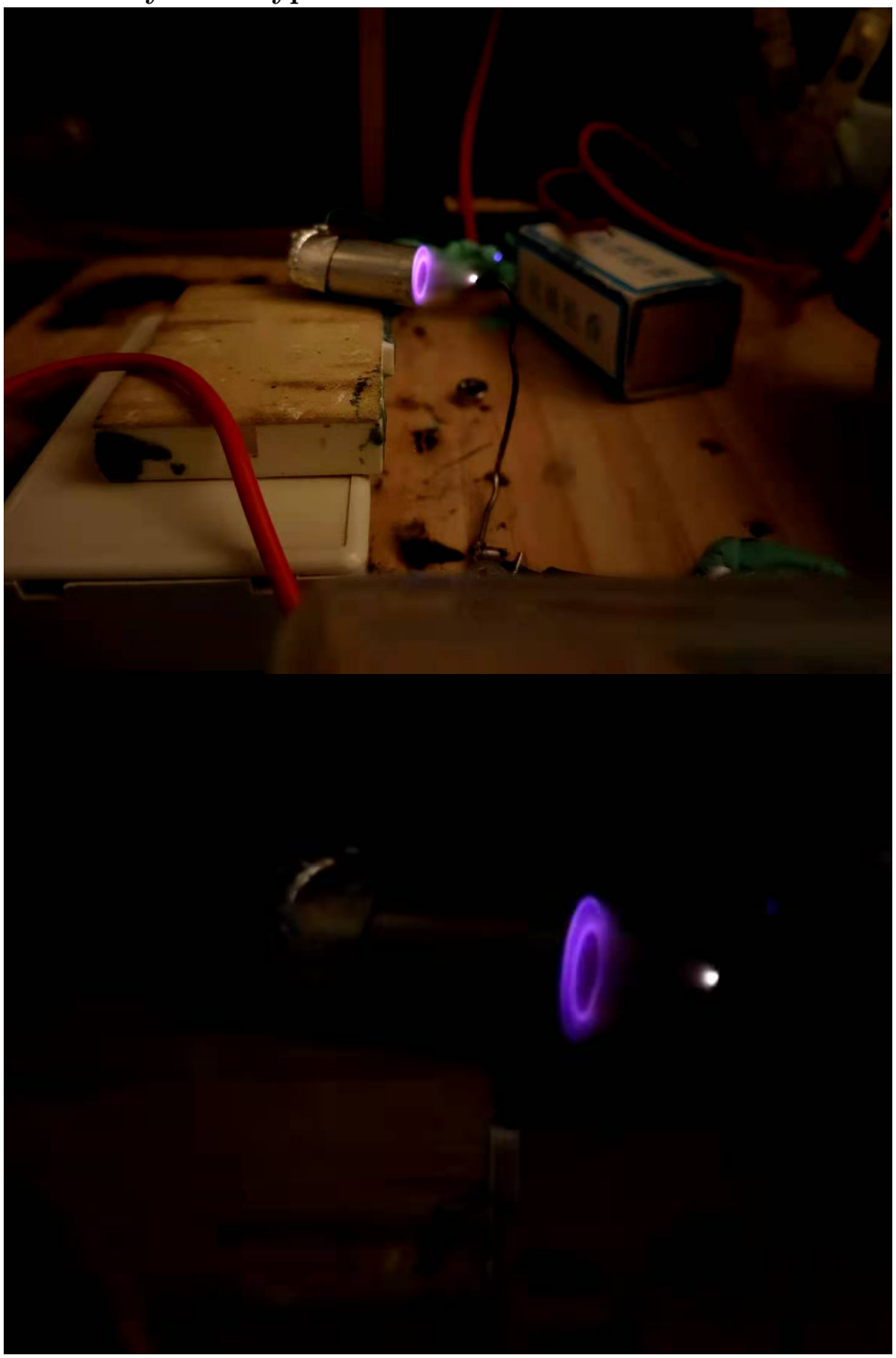

Figure 12: Early prototype thruster with a single tube / electrode pair.

9.4 CAD design and thruster dimensions

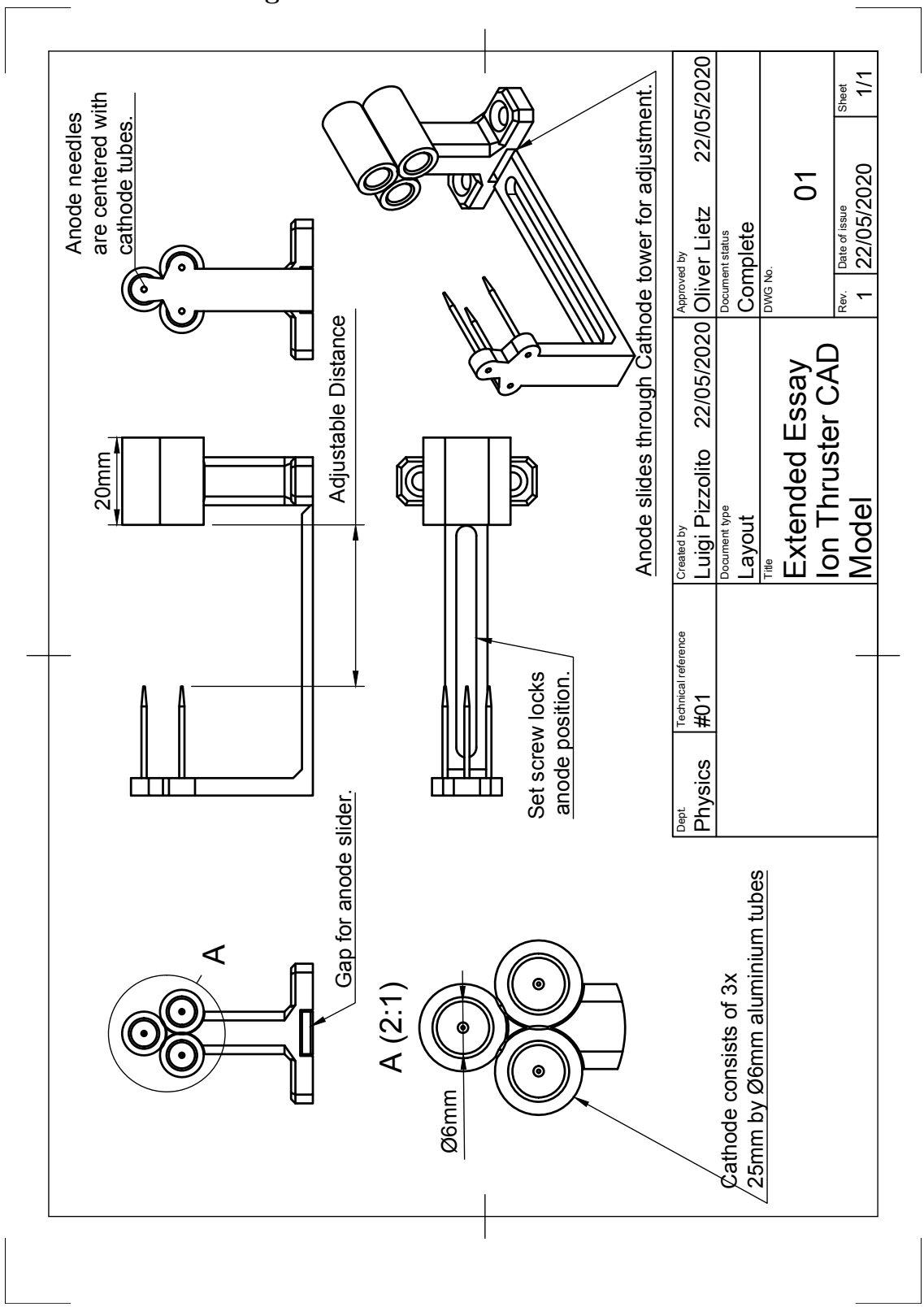

Figure 13: CAD design and dimensions for thruster

9.5 Thruster's physical construction

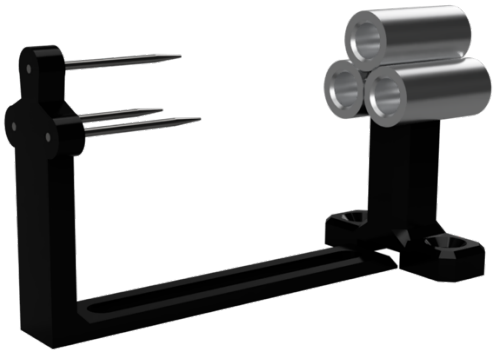

Figure 14: Preview render of CAD model

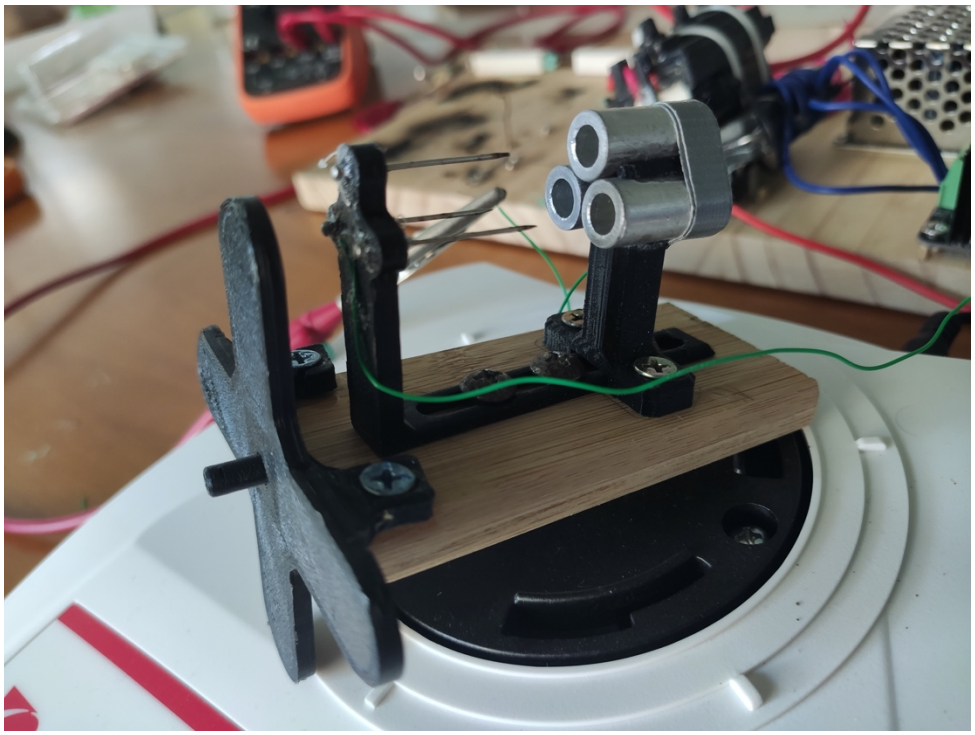

Figure 15: Photo of assembled thruster after 3D printing parts

Notes on Construction:
A piece of bamboo and timber were used to create the bases for the thruster and the power supply board respectively. Screws are all ∅3mm by 10mm self-tapping wood screws with either tapered or flat heads. Anode wire is held in place by transparent adhesive, cathode wire is held in place by duct tape. Electrode wires are 30AWG wire-wrapping-wire.

9.6 Detailed materials and equipment list

Tools	**Specification**	**Use**
Scale Balance	±0.01g	Measuring thrust.
Digital Multi Meter	±00.01mV	Measuring voltage.
Anemometer	±0.01ms^{-1}	Measuring wind speed.
Digital Callipers	±00.01mm	Measuring electrode gap.
Timer	±10s	Timing trials.
Phillips Screwdriver	Suitable for ∅7mm head sized screws.	Locking electrode support position.
Retort Stand	With clamps/connectors.	Holding up weight of wires from scale.
Digital Hygrometer	±1RH%	Measuring air RH.
Equipment/Materials	**Specification**	**Use**
AC Lead	Min. Power 60W	Power to SMPS.
Switch Mode Power Supply	12V 5A	Power to ZVS driver.
ZVS Driver	-	Power to ZVS transformer.
ZVS Transformer	-	HV generator.
Ceramic Resistors	2 units, 5Ω 10W	Current sensing.
Banana wires w/ Alligator Clips	2 units to DMM, 2 units to Thruster.	Making connections.

Metal Tubes	3 units, aluminium, outer ∅8mm, inner ∅6mm, cut to 25mm length.	Cathode.
Metal Needles	3 units, sewing pins, ∅0.8mm by 25mm.	Anode.
Metal Screws	10 units, self-tapping for wood. ∅3mm threads, ∅7mm Philips head.	Mounting.
3D Printed Parts	Anode tower, cathode tower, cathode tube separators and mount.	Electrode support structures and scale mounting.
Scrap Wood Pieces	Adjust to needs.	Base for power supply and thruster.

Table 10: Summary of tools, equipment and materials needed.

9.7 Sample empty data collection table

Distance between electrodes (mm)(±0.01)	Weight (g) (±0.01)				DMM Voltage (mV) (±0.01)				Wind Speed (ms^{-1}) (±0.01)			
	T1	**T2**	**T3**	**T4**	**T1**	**T2**	**T3**	**T4**	**T1**	**T2**	**T3**	**T4**
20.00												
18.75												
17.50												
16.25												
15.00												
13.75												
12.50												
11.25												
10.00												
Arc Distance(mm±0.01)												

Table 11: Empty data collection table.

9.8 Arc during experiment

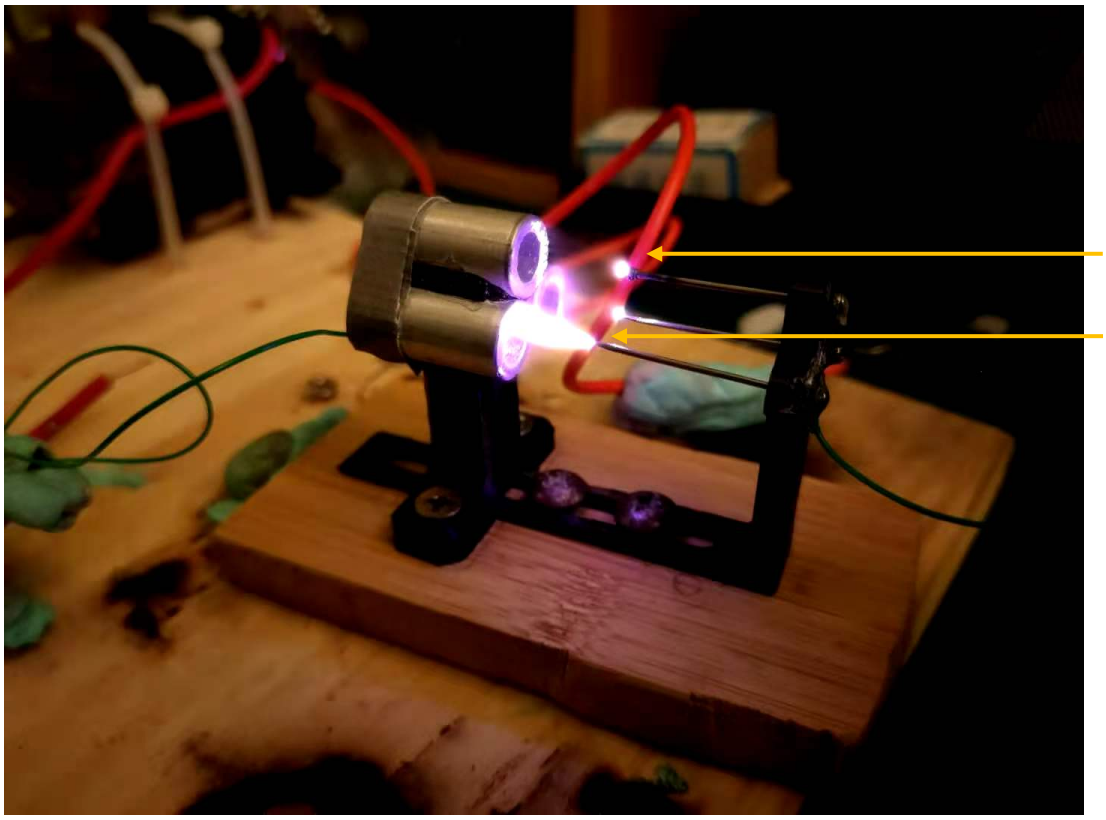

Figure 16: Arc during experiment when electrode separation was too small.

9.9 Additional Graphs

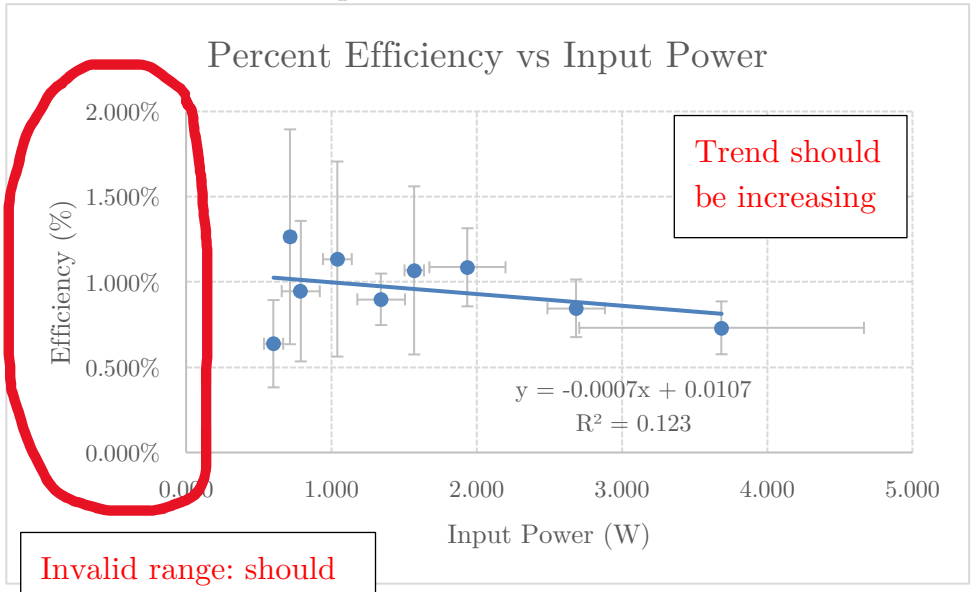

Graph 6

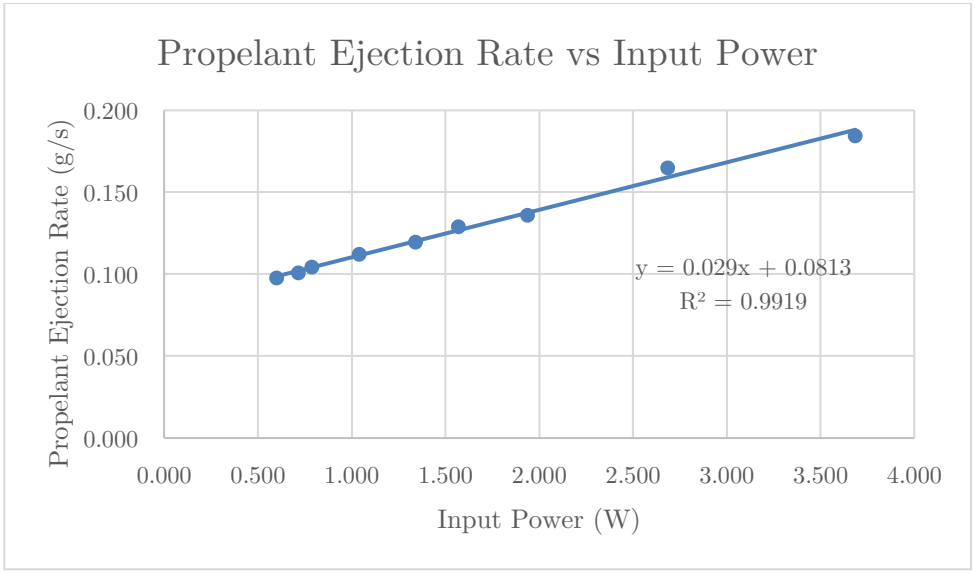

Graph 7

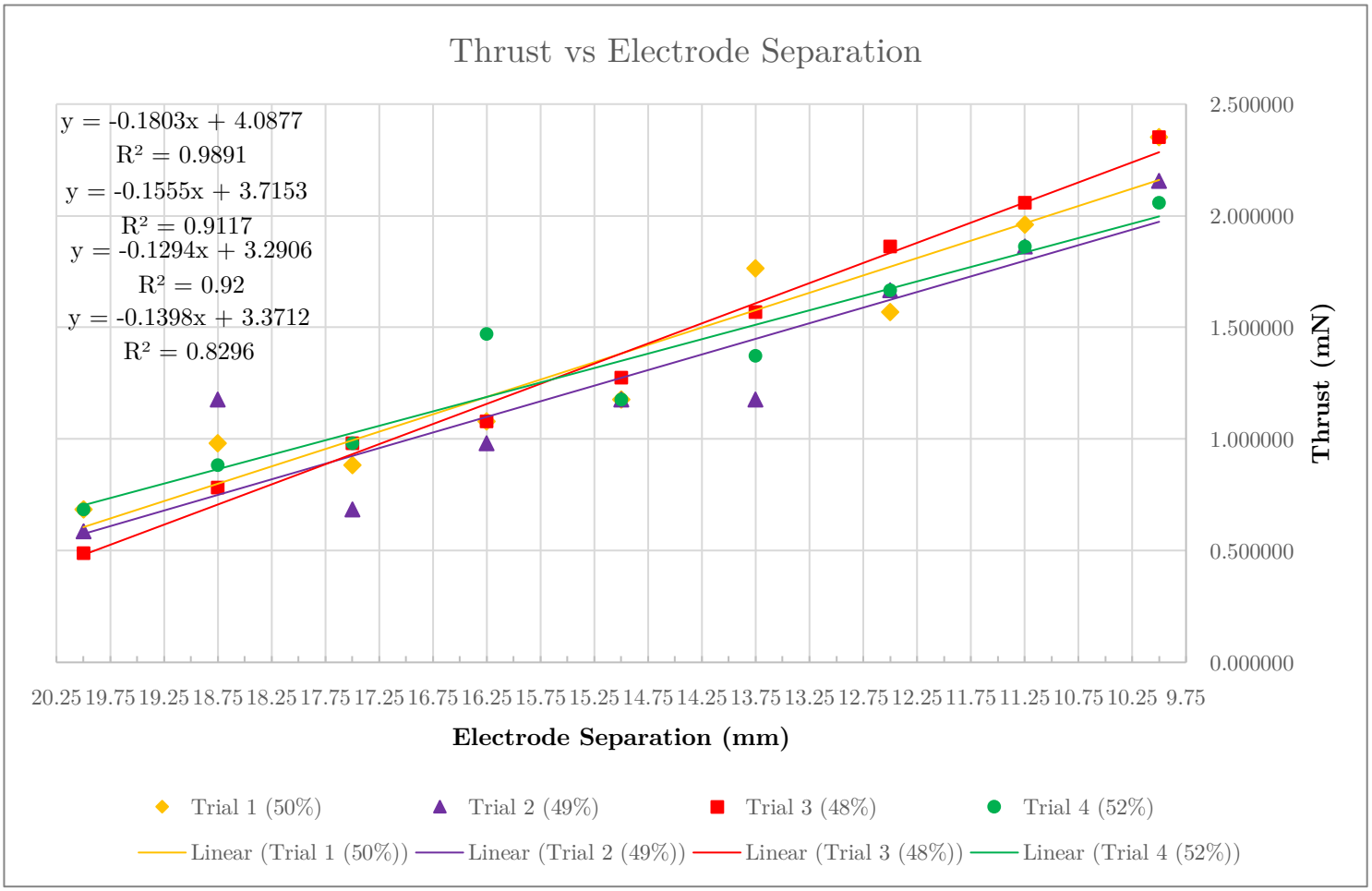
Thrust vs Electrode Separation
y = -0.1803x + 4.0877
R² = 0.9891
y = -0.1555x + 3.7153
R² = 0.9117
y = -0.1294x + 3.2906
R² = 0.92
y = -0.1398x + 3.3712
R² = 0.8296
2.500000
2.000000
1.500000
1.000000
0.500000
0.000000
Thrust (mN)
20.25 19.75 19.25 18.75 18.25 17.75 17.25 16.75 16.25 15.75 15.25 14.75 14.25 13.75 13.25 12.75 12.25 11.75 11.25 10.75 10.25 9.75
Electrode Separation (mm)
Trial 1 (50%)
Trial 2 (49%)
Trial 3 (48%)
Trial 4 (52%)
Linear (Trial 1 (50%))
Linear (Trial 2 (49%))
Linear (Trial 3 (48%))
Linear (Trial 4 (52%))

Graph 8

9.10 Corona discharge of different sharp electrodes

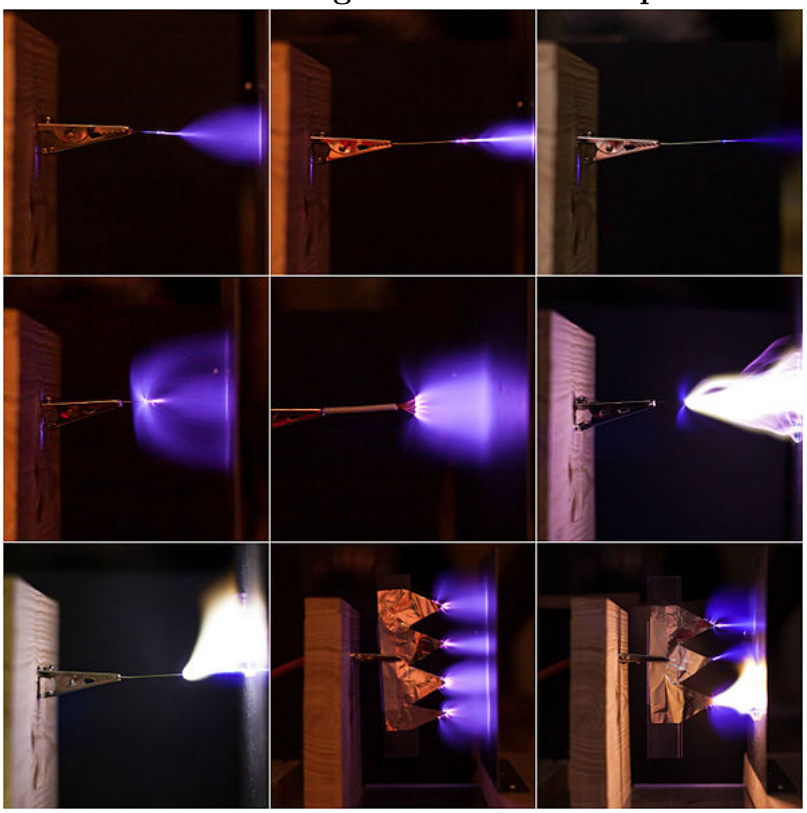

Figure 17: Corona discharge showing the local electric field strengths for differently shaped sharp electrodes (Croatian, 2014).

9.11 Shots of the thruster in operation

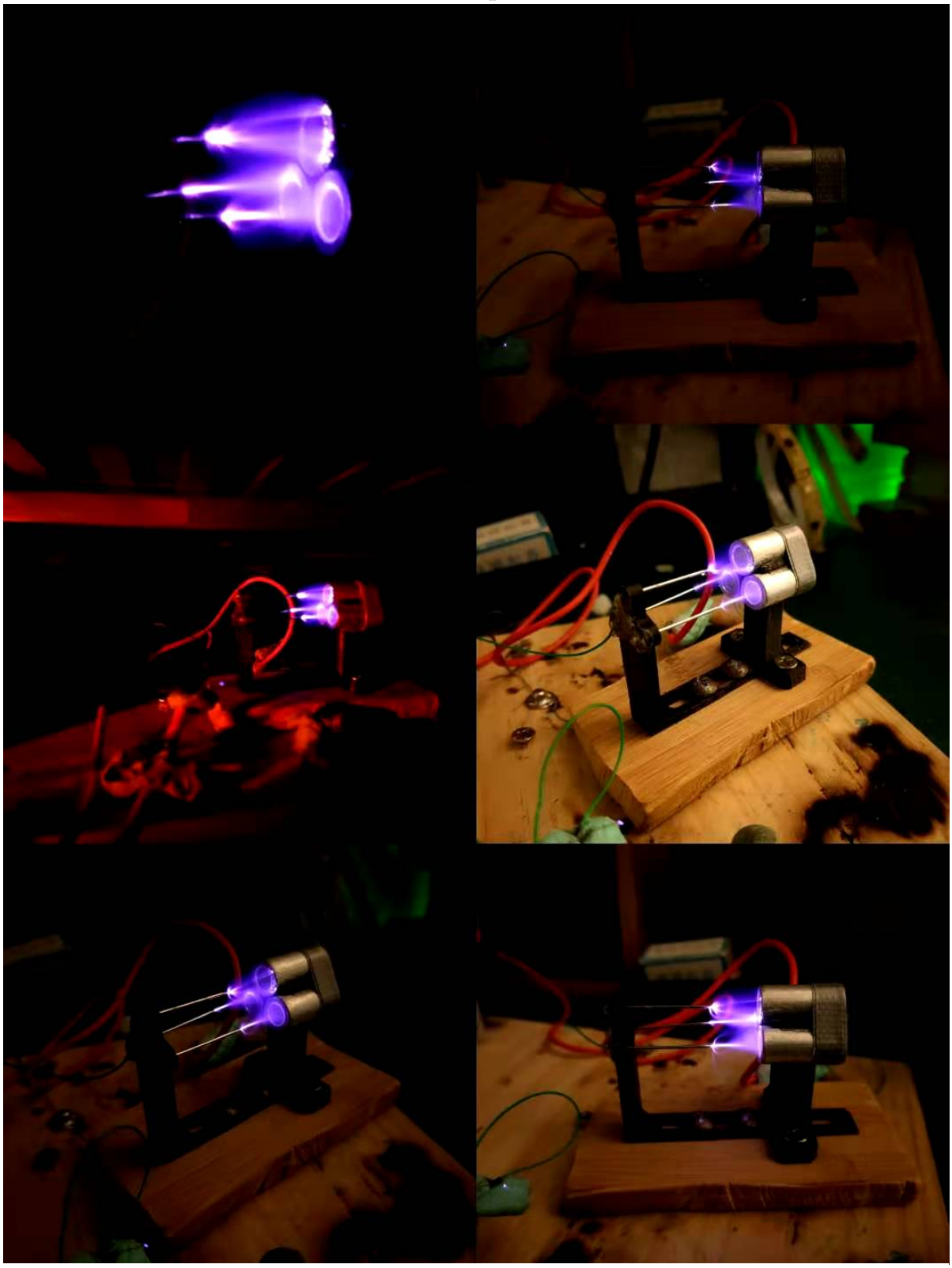

Figure 18: Thruster in operation.